Elucidating the Impacts of COVID-19 Lockdown on Air Quality and Ozone Chemical Characteristics in India

Behrooz Roozitalab[1,2], Gregory R. Carmichael[1,2], Sarath K. Guttikunda[3], Maryam Abdi-Oskouei[4]

[1]Center for Global and Regional Environmental Research, University of Iowa, Iowa City, IA, USA

[2]Chemical and Biochemical Engineering, University of Iowa, Iowa City, IA, USA

[3]Urban Emissions, New Delhi, India

[4]University Corporation for Atmospheric Research (UCAR), Boulder, CO, USA

Corresponding authors: B. Roozitalab (behrooz-roozitalab@uiowa.edu) and G. R. Carmichael (gcarmich@engineering.uiowa.edu)

Key Points:

- Both emission and meteorological changes led to cleaner air during the lockdown period in April 2020 in India.
- Ozone formation in most parts of India is within NOx-limited photochemical regime.
- Carbon monoxide, formaldehyde, isoprene, acetaldehyde, and ethylene are the major volatile organic compounds of ozone formation in India.

Abstract

India implemented stay-at-home order (i.e. lockdown) on 24 March 2020 to decrease the spread of novel COVID-19, which reduced air pollutant emissions in different sectors. The Weather Research and Forecasting model with Chemistry (WRF-Chem) was used to study the changes in air pollutants during the lockdown period in 2020 compared with similar period in 2019. We found that both meteorology and lockdown emissions contributed to daytime $PM_{2.5}$ (-6% and -11%, respectively) and ozone (-6% and -8%, respectively) reduction averaged in April 2020 in the Indo-Gangetic Plain. However, the ozone concentration response to reductions in its precursors (i.e. NO_2 and VOCs) due to the lockdown emissions was not constant over the domain. While ozone concentration decreased in most parts of the domain, it slightly increased in major cities like Delhi and in regions with many power plants. We utilized the reaction rates information in WRF-Chem to study the ozone chemistry. We found carbon monoxide, formaldehyde, isoprene, acetaldehyde, and ethylene as the major VOCs that contribute to the ozone formation in India. We used the ratio of chemical loss of radicals with radicals and NOx, and its corresponding formaldehyde to NO_2 ratio (FNR) to find the ozone chemical regimes. Using the upper limit of FNR transition region (1.3), we found that most parts of India are within NOx-limited regime while urban regions and the regions with many power plants are in a VOC-limited regime. As a result, policy makers should study the characteristics of a region before implementing mitigation strategies.

1. Introduction

While COVID-19 virus is a global disaster in terms of its health and economy damages, it provides a unique opportunity in earth system sciences (Gorris et al., 2021). As many countries initiated stay-at-home orders (hereafter called lockdown) in early 2020 to control the spread of the virus, anthropogenic air pollutant emissions started to decline in different sectors (Doumbia et al., 2021). While many studies had used numerical models to understand the impacts of stringent future emission control "scenarios" on air quality (Amann et al., 2020), worldwide lockdowns introduced a scenario accompanied by actual observational data. As a result, numerous studies have studied the changes in air pollution using ground measurements (e.g. Shi and Brasseur (2020)) and satellite data (e.g. Goldberg et al. (2020)). An exhaustive review on these studies can be found in Gkatzelis et al. (2021). However, these data have spatial or/and temporal gaps. In order to utilize the models, some studies used available activity data (e.g. Doumbia et al. (2021)) or inverse modeling (e.g. Souri et al. (2021)) to update emission inventories.

Air pollution is a concerning issue in India due to its large health and environmental impacts (Ghude et al., 2014; HEI, 2018). While even extreme air pollution events are not unusual in India (Roozitalab et al., 2021), clean air due to the lockdown was unusual and attracted people and media's attention (Gupta, 2020). In India, the lockdown officially started on 24 March 2020 and continued in four phases until the end of May 2020. While residential and power sectors emissions did not show large changes, large emission reductions were reported in other sectors such as transportation (Beig et al., 2021). This reduction in emissions resulted in different changes in air quality over India. Relatively short lifetime of NO_2 makes it a suitable tracer of local NO_x emissions (Goldberg et al., 2019). Figure 1 shows the tropospheric column NO_2 concentration in April 2019 and 2020 over northern India retrieved from the TROPOspheric Monitoring Instrument (TROPOMI) satellite data. Lower values in April 2020 compared with 2019 indicate reductions in NOx emissions in most parts of India except the thermal power plant regions. For example, NO_2 concentrations showed large reductions over Delhi and other urban regions due to the lower activities in transportation sector. However, the demand for electricity showed small changes during the lockdown period; NO_2 concentrations did not change very much over the thermal

power plants region (ESA, 2020). Other studies using TROPOMI and Ozone Monitoring Instrument (OMI) satellites and ground measurements data confirmed these changes (Biswal et al., 2020).

Many studies used measurement data and studied the changes in air pollutant concentrations in Indian regions during different phases of the lockdown period (Jain & Sharma, 2020; V. Kumar et al., 2020; Kumari & Toshniwal, 2020; Mahato et al., 2020; Selvam et al., 2020; Singh et al., 2020). While the studied periods are different in each study, the conclusion was solid. All of them found significant reductions in $PM_{2.5}$ and NO_2 concentrations when compared to pre-lockdown period or previous years. A limited number of studies have also investigated the lockdown emission effects in India. Zhang et al. (2021) used WRF-CMAQ model to study the pre-lockdown-to-lockdown air quality changes in India, between 21 February and 24 April 2020, by decreasing the emissions in industrial (82%), transportation (85%), and energy (26%) sectors during the lockdown period. They found that air quality improved over India for all the pollutants with some exceptions of MDA8 ozone for some urban areas. Dumka et al. (2021) used the WRF-CHIMMERE model and simulated significantly lower $PM_{2.5}$ and NO_2 concentrations over India during the lockdown period (25 March and 17 May 2020) compared with the pre-lockdown period by completely excluding traffic and industrial sectors from the emission inventory. Gaubert et al. (2020) used CESM2 model and adjusted emission based on the work by Doumbia et al. (2021) to study the meteorological and lockdown emission impacts on the secondary atmospheric pollutants during the lockdown period over the world. They found that the lockdown emissions reduced ozone in India, while meteorology had both decreasing and increasing effect on ozone concentration. In general, the above-mentioned studies found unexpected changes in ozone concentrations. While large reductions in NO_2 concentration, as its' precursor, were found, lower reductions were reported in ozone concentrations (Zhang et al., 2021). Moreover, some enhancements in observed ozone concentrations compared with the pre-lockdown period were found (Kumari & Toshniwal, 2020; Mor et al., 2021). Similarly in global scale, Miyazaki et al. (2020) found that NOx emission reductions due to the COVID-19 lockdowns led to about 2% reduction in the global tropospheric ozone burden, while surface ozone concentrations increased in some regions (Shi & Brasseur, 2020; Sicard et al., 2020).

Different response of ozone to its precursors' changes is due to its complicated chemistry. Chen et al. (2020) studied the sensitivity of ozone formation to its precursors and aerosol loading in Delhi. They found that a reduction by more than 65-80% in NOx emissions alone was needed to reduce the ozone concentration, whereas VOC emission reductions were the efficient control strategy. On the other hand, the effects of meteorology should also be considered when studying the differences in concentrations between 2020 and previous years. Gkatzelis et al. (2021) found only about one-third of all the global studies on the effects of COVID-19 accounted for impacts of changing meteorology. For example, Goldberg et al. (2020) showed that meteorological conditions alone decreased tropospheric column NO_2 concentration by a median of 21.6% in the United States (US) in 2020 compared with 2019. Different meteorology can also change the amounts of biogenic emissions, dust emissions, and biomass burning emissions. As a result, a modeling study is required to investigate the impacts of meteorology and lockdown emissions on the air quality during the lockdown period. Furthermore, numerous modeling studies have been performed over India with the primary focus on PM (Garaga et al., 2018), while only a few of them have studied ozone (Luke Conibear et al., 2018; Ghude et al., 2016; Kota et al., 2018; R. Kumar et al., 2012; Sharma et al., 2017).

The objectives of this study are to understand 1) how the meteorology and COVID-19 lockdown emissions affected air quality in northern India and 2) how ozone precursor's emissions contributed to ozone formation in India. To achieve these objectives, we used the regional Weather Research and Forecasting Model with Chemistry (WRF-Chem) version 4 to simulate the air quality during March and

April in 2019 and 2020. We also utilized the Integrated Reaction Rate (IRR) capability in this version to understand how ozone formed in different regions (i.e. urban, non-urban, and a thermal power plant region) in India and how it changed during the lockdown period. To account for emission changes during the COVID-19 lockdown period, we used the adjustment factors proposed by Doumbia et al. (2021).

The paper is organized as follows. First, we provide a description of the WRF-Chem model and adjustment factors used to account for the lockdown period emissions, and evaluate the modeling results against ground measurements data in 2019 and 2020. Then, we study the effects of meteorology and lockdown emissions on air quality using different modeling experiments. Finally, we use the IRR and study the ozone chemistry in different regions in India and provide a summary of the findings.

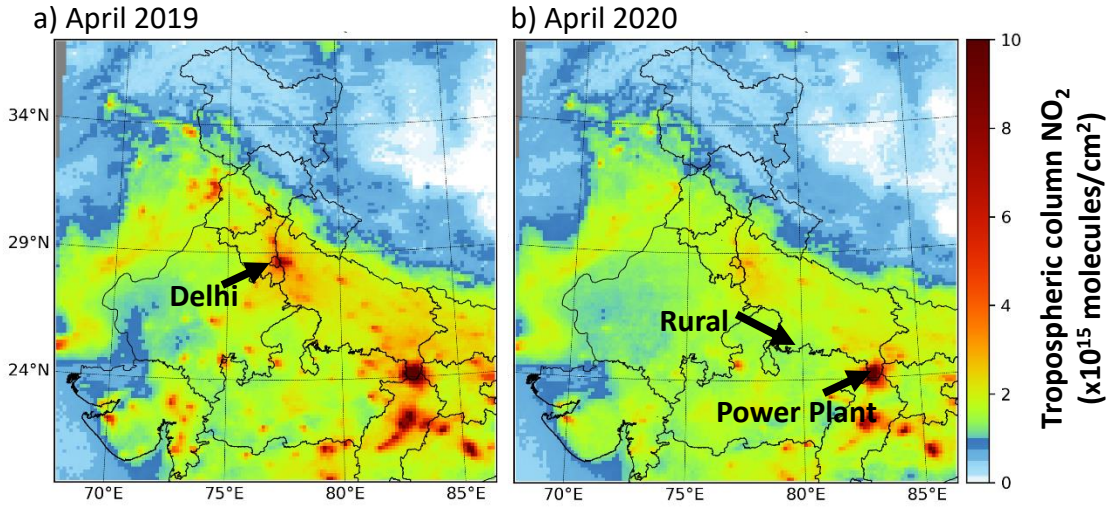

Figure 1 Tropospheric column NO_2 concentrations over the WRF-Chem modeling domain averaged for April a) 2019 and b) 2020 retrieved from TROPOMI on board the Copernicus Sentinel-5 Precursor satellite. The three regions used for process analysis has been marked and also shown on Figure S1. The quality assurance more than 0.5 was used.

2. Methods:

2.1. WRF-Chem modeling

WRF-Chem model version 4.0 was used in this study in order to utilize its new IRR capability (Grell et al., 2005; Pfister et al., 2019). We used a single domain, centered over Delhi, which covered the Indo-Gangetic Plain (IGP) and central India with a 15 km x 15 km resolution and 39 vertical layers (Figure 1; location of the IGP is shown in Figure S6). The Model for Ozone and Related chemical Tracers, version 4 (MOZART-4) introduced by Emmons et al. (2010) with updates on monoterpenes (Hodzic et al., 2015) and isoprene oxidations (Knote et al., 2014) was selected as the gas phase chemistry mechanism (More information on the evolution of the MOZART mechanism can be found in Emmons et al. (2020)). For aerosol representation, the four-bin MOdel for Simulations Aerosol Interactions and Chemistry (MOSAIC-4bin) introduced by Zaveri et al. (2008) with updates for Secondary Organic Aerosol (SOA) formation (Hodzic & Jimenez, 2011) was selected.

Initial and boundary condition (IC/BC) for meteorological fields were provided by National Center for Atmospheric Prediction Global Forecasting System Final Analysis (NCEP GFS-FNL) data (https://rda.ucar.edu/datasets/ds083.2/, last access: 20 December 2020). For Chemical IC/BC, we used the

Whole Atmosphere Community Climate Model (WACCM) outputs (*Whole Atmosphere Community Climate Model (WACCM) Model Output*, 2020). We reinitialized the model every 30-hours and updated meteorological IC/BC and chemical boundary conditions but used the chemical initial condition from the previous cycle. The re-initialization for every cycle started during nighttime at 1800 UTC (2330 Local Time (LT)) and the first 6 hours were discarded as spin up following Abdi-Oskouei et al. (2018). The simulation period included March and April in 2019 and 2020, while we primarily focus on April results. The details of other configuration options can be found in Roozitalab et al. (2021).

We used the Hemispheric Transport of Air Pollution emission inventory (HTAP v2.2) 0.1x0.1 degree gridded monthly-averaged for each sector as our base anthropogenic emission inventory (Janssens-Maenhout et al., 2015). The speciation provided by Emissions of atmospheric Compounds and Compilation of Ancillary Data (ECCAD) database for Non Methane Volatile Organic Carbons (NMVOCs; hereafter NMVOCs refer to VOCs except Methane and CO and VOCs refer to their inclusion), which is based on ratios in the RETRO project (https://permalink.aeris-data.fr/HTAPv2, last access: 20 December 2020). Moreover, the mapping between the ECCAD NMVOCs and model emitted species are provided in Table S1 (personal communications with Louisa Emmons, NCAR). In this study, we arbitrarily chose three regions representing an urban, a rural, and a power plant region when analyzing the ozone chemistry (Figure 1). The urban region contains the greater Delhi region (hereafter called Urban), the rural area contains a non-urban region with low population density in the border of Uttar Pradesh and Madhya Pradesh states (hereafter called Rural), and the power plant region covers an area with high emission thermal power plants (hereafter called Power). To keep the regions comparable with each other, each region includes a set of 4x5 grid cells in the model (~4500 km^2; Figure S1). Hereafter, we also call the Indian regions of the domain as India. The amount of HTAP v2.2 emissions for different species over these defined regions for the month of March and April are shown in the supporting information (Table S2 and Table S3). Urban had the highest emissions for all the species except for SO_2. SO_2 emissions were higher in Power. The amount of NOx emission was close in Urban and Power regions. On the other hand, NMVOC emissions were very low in Power and Rural. Emissions in April were lower than March for all the regions; however, this difference was very small for Rural as the emissions were originally low.

To consider emission reductions due to the lockdown in 2020, we used the adjustment factors (AFs) provided by Doumbia et al. (2021). Doumbia et al. (2021) estimated the global gridded AFs based on the change of activity data for each sector with respect to a five-week period starting on January 2020. Figure 2 shows the daily change of emissions for a) India, b) Urban, c) Power, and d) Rural. It shows a small fluctuation in emissions until 24 March (as adjusting factors are with regard to January), with a dramatic change afterwards due to initiation of the lockdown. The lockdown had the largest impact on NO_x emission with greater than 40% reduction averaged over India. The emissions of SO_2 also showed large reductions with smaller reductions for NMVOCs and CO. Black carbon did not change very much over India, while Organic Carbon (OC) increased after the lockdown due to increased fuel consumption for residential sector (Yadav et al., 2020). The total changes in emission in each region depends on both the AFs and the amount of emission from each sector in that region. Urban showed similar emission reductions for both NOx and NMVOCs as for India. Reduction in emission of NMVOC was lower than NOx in Power and Rural. Moreover, the amount of emission change was different as well. For example, NOx emissions reduced by up to 60%, 50%, and 30% in Urban, Rural, and Power, respectively. On the other hand, OC and black carbon decreased in Urban, while increased over other regions. Figure 2 (e, f) also shows the maps of averaged emission reductions in April 2020 for NMVOC and NOx. Although these results are qualitatively consistent with results in Gaubert et al. (2020), there are some quantitative differences, primarily due to different base emission inventory and considered regions.

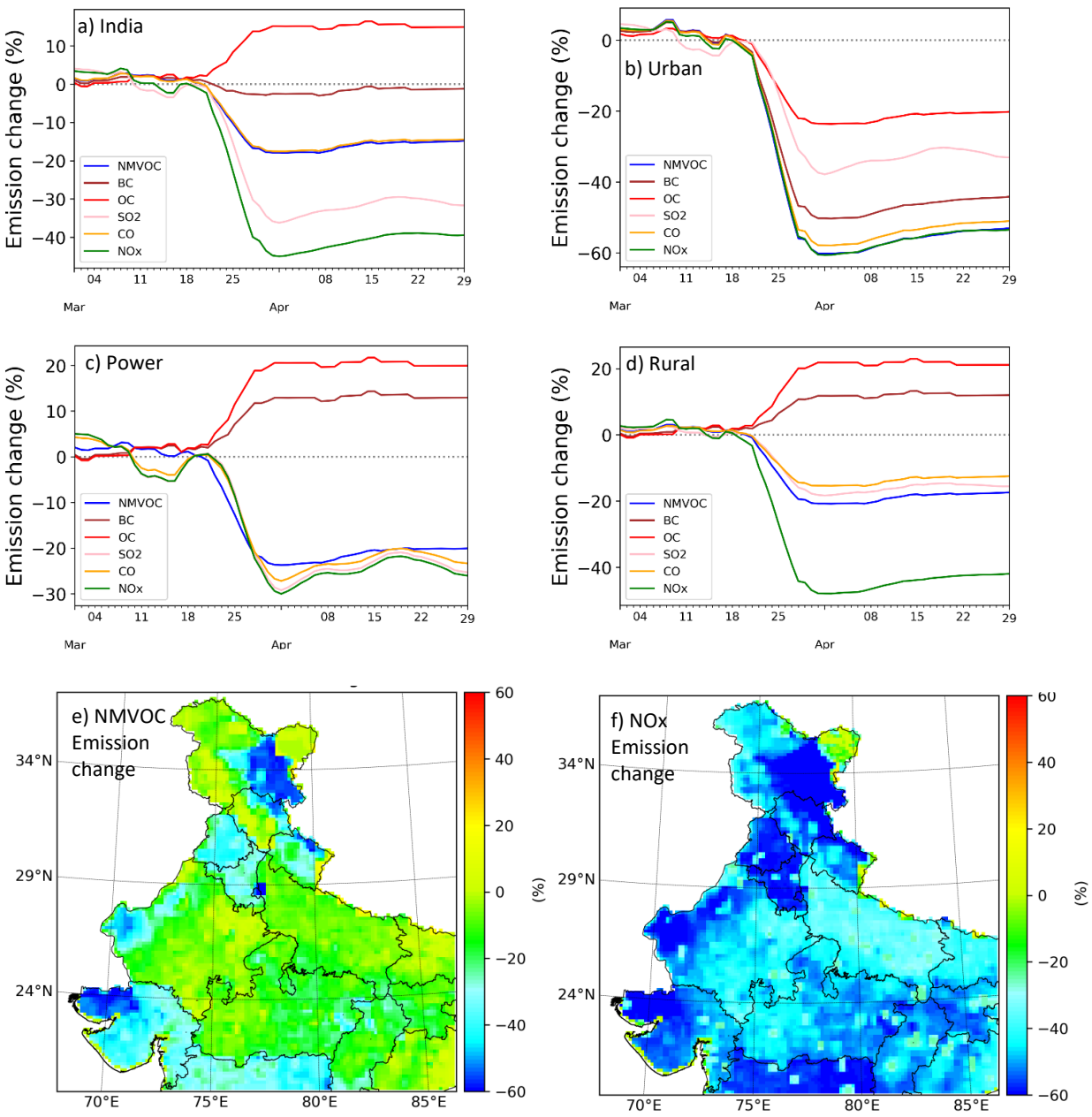

Figure 2 Daily Emission change due to AF applied on HTAP v2.2 emissions averaged in a) India, b) Urban, c) Power, and d) Rural (X-axis shows the days in March and April and Y-axis range is different for each subplot). Map of emission changes of e) NMVOC and f) NOx averaged in April 2020.

The Fire Inventory from NCAR, version 2.2 (FINN v2.2) based on MODIS fire detections was used as the biomass burning emission inventory (Wiedinmyer et al., 2011). Comparing the fire emissions between 2019 and 2020 during the studied period showed lower total emissions in 2020 (Figure S2), with most of the fires over central parts of the domain. However, it also showed that some days in 2020 (e.g. 16 April) had much larger emissions compared with 2019. We also used the online Model of Emissions of Gases and Aerosols from Nature (MEGAN v. 2.0.4) as the biogenic emission inventory (Guenther et al., 2006). MEGAN emissions changed between years 2019 and 2020 as they are based on meteorological fields (i.e.

temperature). For Dust emissions, we used the online Goddard Global Ozone Chemistry Aerosol Radiation and Transport (GOCART) mechanism.

To study the response of air quality to both meteorological and emission forcings, we performed four simulations (Table 1). It should be noted the we considered all emission sources that are directly (i.e. biogenic and wind-blown dust) and indirectly (biomass burning) related to the meteorology as meteorological forcings. The reason is that the lockdown anthropogenic emissions' adjustments do not directly affect these sources. In the 2019BAU scenario, all the year-dependent input data including chemical and meteorological IC/BC, and biomass burning emissions were from 2019. As a result, online biogenic and dust emissions also followed 2019 meteorology. Moreover, we used HTAP v2.2 emission inventory as Business As Usual (BAU) anthropogenic emission in 2019BAU. Following the same logic, 2019COVID means 2019 year-dependent input data, while anthropogenic emissions were adjusted based on the multiplication of HTAP v2.2 and AFs for each sector. Similarly, 2020BAU was based on 2020 year-dependent input data and BAU anthropogenic emission, while 2020COVID used adjusted emissions. These four scenarios provide an opportunity to look at the effects of meteorology, emissions, and their combined effects on air quality over the domain.

Table 1 List of scenarios performed in this study

Scenario	Meteorology	Anth. Emission	Biomass Burning Emission	Biogenic Emission	Dust Emission	Initial/Boundary Condition
2019BAU	2019	HTAP v2.2	2019	2019	2019	2019
2019COVID	2019	HTAP v2.2 adjusted with AF	2019	2019	2019	2019
2020BAU	2020	HTAP v2.2	2020	2020	2020	2020
2020COVID	2020	HTAP v2.2 adjusted with AF	2020	2020	2020	2020

2.2. Model evaluation

We evaluated the performance of the model compared with ground measurements and global reanalysis data. Scenarios 2019BAU and 2020COVID should represent the real states of the atmosphere for years 2019 and 2020, respectively. In the following model evaluation discussion, the model for 2019 refers to 2019BAU and the model for 2020 refers to 2020COVID results. For meteorological fields, we compared the model with the Modern-Era Retrospective analysis for Research and Applications, Version 2 (MERRA-2) data (Bosilovich et al., 2015). Hourly statistics for a location in Delhi (28.6 N, 77.19 E) showed 2-m temperature (T_{2m}) mean error (ME) of 2.9 °C and 3.5°C in 2019 and 2020, respectively, and 10-m wind speed (WS_{10m}) of 1.3 m/s and 1.3 m/s in 2019 and 2020, respectively. The root mean squared error (RMSE) for T_{2m} was 3.4 °C and 4.1 °C in 2019 and 2020, respectively. The RMSE for WS_{10m} was 1.7 m/s and 1.6 m/s for 2019 and 2020, respectively. These are comparable with Zhang et al. (2021) values when modeling the pre-lockdown and lockdown period in India. The model satisfied the wind speed ME goal of 2.0 m/s, while overestimated temperature ME goal of 2.0 °C, proposed by Emery et al. (2001). The model simulated the daytime (1000-1700 LT) T_{2m} peaks but overestimated nighttime values (Figure S3). Figure 3 shows the averaged hourly T_{2m} over the domain for April 2019 and 2020 in the model (re-gridded to MERRA-2 resolution) and MERRA-2. The model captured the general spatial

pattern of temperature in both 2019 and 2020. However, the model was biased low over most parts of India in 2019. On the other hand, the model was biased high over the IGP and biased low over central India in 2020. It also shows that the model was biased high over the western parts of the IGP in both 2019 and 2020. Comparing WS_{10m} also indicated the ability of the model to capture the spatial pattern, while the model was biased low most of the time in Delhi (Figure S4). The differences in the meteorology can affect the air quality by changing the natural emission sources (e.g. dust and biogenic emissions). Furthermore, the dynamics of the atmosphere (e.g. boundary layer height and wind) change how the air pollutants disperse and transport in the atmosphere.

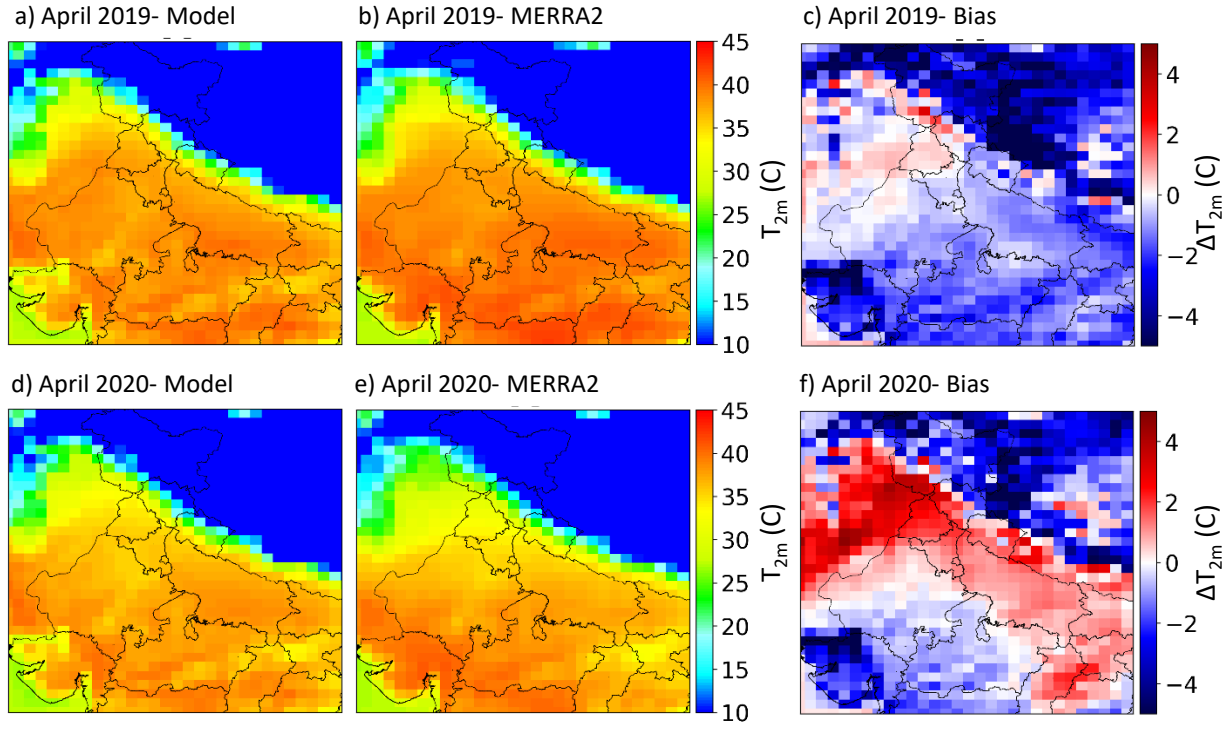

Figure 3 Averaged hourly 2-m temperature in April 2019 (top row) and 2020 (bottom row) in the WRF-Chem model (left column), MERRA-2 (middle column), and their difference (right column).

We used the hourly ground measurements air pollutant concentrations data in Delhi collected by the Central Pollution Control Board (CPCB) to evaluate the air quality in years 2019 and 2020. Other than the original quality control filters applied by the CPCB (https://cpcb.nic.in/quality-assurance-quality-control/, last access: 02/23/2021), we applied four additional filters (Jena et al., 2020; Singh et al., 2020). First, we removed the stations with all zero or not-a-number (i.e. NAN) values. Second, we removed the stations with no variation, in which the standard deviation (STD) of the data was less than five percent of its mean. Third and fourth, we removed the outlier values, in which the difference between two consecutive hours was more than 100 units (except for carbon monoxide (CO), for which we used a cut-off of 300 µg/m3) or the difference between each value and the mean value was higher or lower than 3xSTD.

The model evaluation statistics for $PM_{2.5}$, ozone, NO_2, and CO during April 2019 and 2020 were calculated for daytime (1000-1700 LT) and 24-hour average (i.e. daily) period and are provided in the supporting information (Table S4 and Table S5). The normalized mean bias (NMB) for daily $PM_{2.5}$ was -31% and -17% in April 2019 and April 2020, respectively. Zhang et al. (2021) simulated the period

between 21 February and 23 March in 2020 and reported $PM_{2.5}$ mean normalized bias (MNB) of -16% in Delhi. Roozitalab et al. (2021) reported NMB of -17% in their best experiment for modeling $PM_{2.5}$ in an extreme pollution event in November 2017. The model overestimated daytime ozone concentrations with NMB of 43% and 78% in April 2019 and April 2020, respectively. On the contrary, the model was biased low for NO_2 by daytime NMB of -35% and -47% for April 2019 and April 2020, respectively. The model underestimated daytime CO concentrations by NMB of -67% and -64% for April 2019 and April 2020, respectively. Kota et al. (2018) modeled air quality in India in 2015 and reported NMB of 53%, -33%, and -54% for ozone, NO_2, and CO, respectively, in Delhi. Other studies have also reported overestimation of simulated ozone concentrations over Delhi (Luke Conibear, 2018; Ghude et al., 2016; R. Kumar et al., 2012; Pommier et al., 2018). On the contrary, Sharma et al. (2017) underestimated diurnal ozone by 16 ppb in Delhi. Furthermore, Zhang et al. (2021) slightly underestimated ozone in Delhi by MNB of -4%. They also reported MNB of -51% and -59% for NO_2 and CO, respectively. Overall, the model performance for $PM_{2.5}$ was similar to other studies and daily NMB is within the benchmark criteria of Emery et al. (2017). However, the model was biased low for daytime ozone precursors (NO_2 and CO) concentrations and biased high for daytime ozone mixing ratios.

We explored the extent to which model performance was influenced by the year the emission inventory was based on. The HTAP v2.2 emissions used in these simulations are estimates for 2010. As a result, we performed a set of experiments using the Copernicus Atmosphere Monitoring Service global emission inventory version 4.2 (CAMS v4.2; Granier et al. (2019)). Our analysis indicated that the concentrations and changes in concentrations due to lockdown emissions were close in both CAMS and HTAP emissions (More information can be found in supporting information). As a result, we performed all further analysis in this study based on HTAP anthropogenic emission inventory. Figure 4 shows the averaged daytime $PM_{2.5}$, NO_2, and ozone concentrations measured (left panels) and modeled (right panels) between 10 March and 30 April in 2019 (blue colors) and 2020 (red colors) in Delhi. Both measured data and the model showed similar values in 2019 and 2020 between 10 March and around 24 March (before lockdown) accompanied by a drop afterwards (during lockdown). However, the day that concentrations dropped is different between the measured data (22 March) and the model (24 March). Yadav et al. (2020) also reported that the lockdown was not abrupt and had a transition start. Furthermore, the averaged amount that concentrations dropped during the lockdown period (24 March-30 April) in 2020 compared with 2019 was different between measured data and the model. Mean reduction for daytime $PM_{2.5}$ concentrations was 26 µg/m3 in measured data, while the model showed a smaller drop (9 µg/m3). For daytime NO_2, the measured data decreased by 14 µg/m3 (50%), while the modeled outputs decreased by 8 µg/m3 (61%). Vadrevu et al. (2020) also reported 61% reduction in TROPOMI tropospheric column NO_2 concentrations during 25 March and 3 May in 2020 compared with 2019. Daytime ozone mixing ratio also dropped during the lockdown in both measured (10 ppb) and modeled (7 ppb) data. However, 24-hour averaged ozone mixing ratio did not change very much neither in the measured data nor in the model although small fluctuations were observed between years 2019 and 2020 (Figure S5). We will further analyze this behavior in the process analysis section (Section 3.2). Although April 2019 daytime ozone mixing ratios were higher than March 2019, we observed lower daytime ozone mixing ratios in April 2020 compared with March 2020, both in the model and measured data. This may be seen in contrast with what other studies that reported slightly higher ozone in Delhi during the lockdown compared with pre-lockdown period (Jain & Sharma, 2020; Mahato et al., 2020). These differences are primarily due to the methodology and the observed time period. For example, Jain and Sharma (2020) reported an increase in daily ozone while we report the daytime ozone. On the other hand, Mahato et al. (2020) looked at maximum daily 8-hour averaged (MDA8) ozone during two weeks in lockdown period

compared with two weeks in pre-lockdown period and reported less than 1% increase. Overall, the model was able to capture the major responses to the lockdown.

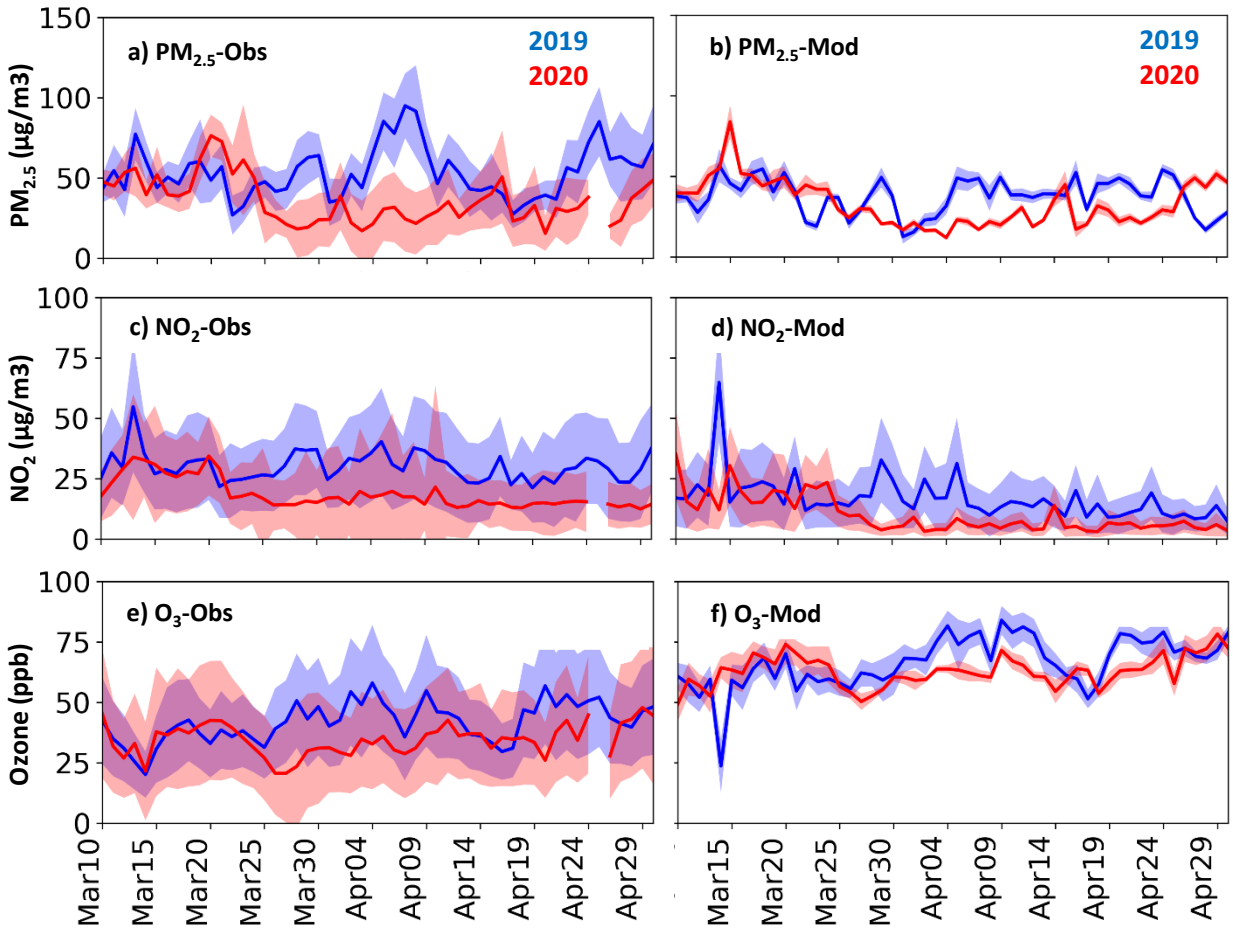

Figure 4 Averaged daytime (1000-1700 LT) $PM_{2.5}$ (top row), NO_2 (middle row), and ozone (bottom row) concentrations measured over CPCB stations in Delhi (left column) and modeled over Urban region (right column) between 10 March and 30 April in 2019 (blue colors) and 2020 (red colors). The shaded regions show ±1STD. The observed data were extracted from the ground measurements data in Delhi, while the modeled data were averaged in the Urban subdomain.

3. Results

3.1. Model responses to Meteorology, Emission, and Combined effects

To compare the air quality during the lockdown period (April 2020) with regards to the previous year, it is important to note that not only emissions but also the meteorology changed. Indeed, meteorology can affect both the transport of the pollution and natural sources emissions (i.e. biogenic and biomass burning emissions). Figure 5 shows the differences in 2-m temperature, biogenic isoprene emission, and biomass burning NOx emission averaged during the daytime over the domain in April 2020 and April 2019. The western IGP had lower temperatures in April 2020 while eastern IGP and the state of Gujarat experienced warmer days. Because of higher temperatures, the online MEGAN module estimated by up to 10% more

biogenic isoprene emissions in eastern parts of the IGP in April 2020. On the other hand, it estimated by up to 10% lower isoprene emissions in western IGP in April 2020. Biomass burning emission in the IGP were lower in April 2020 with small fires in the eastern IGP. Overall, eastern IGP had higher biogenic emissions in April 2020, while biomass burning emissions were lower. In central India, biomass burning emissions were higher in April 2020 compared with April 2019. Due to such changes in meteorology and emissions, the effects of reducing anthropogenic emissions on regional air quality can be different depending on the applied year. Figure 6 shows the effects of emission reductions due to the lockdown in years 2019 (the difference between 2019COVID and 2019BAU scenarios) and 2020 (the difference between 2020COVID and 2020BAU scenarios) on averaged daytime $PM_{2.5}$, NO_x, and ozone in the Urban region. The averaged effect of emission perturbation on changes in daytime ozone concentration was -4.1 ppb and -3.4 ppb in 2019 and 2020, respectively. Similarly, the effect of emission reductions on changes in daytime $PM_{2.5}$ concentration in 2019 was -6.3 µg/m3 and was -5.8 µg/m3 in 2020. For NO_x, the emission perturbation effect were similar in both 2019 and 2020. However, we found large differences in day-to-day comparison. For example, lockdown emissions in 2019 and 2020 decreased daytime $PM_{2.5}$ concentrations in Urban by ~12 µg/m3 and ~7 µg/m3, respectively, on 5 April, which corresponds to ~40% difference due to the year applied. Moreover, the amount of reduction in NO_x mixing ratio on 14 April was different by 46% (15 ppb and 7 ppb in 2019 and 2020, respectively). On the other hand, we also observed contradictory responses on some days. For example, ozone mixing ratios in Urban decreased on 14 April 2019 due to the lockdown emissions, while 2020 data showed an increase.

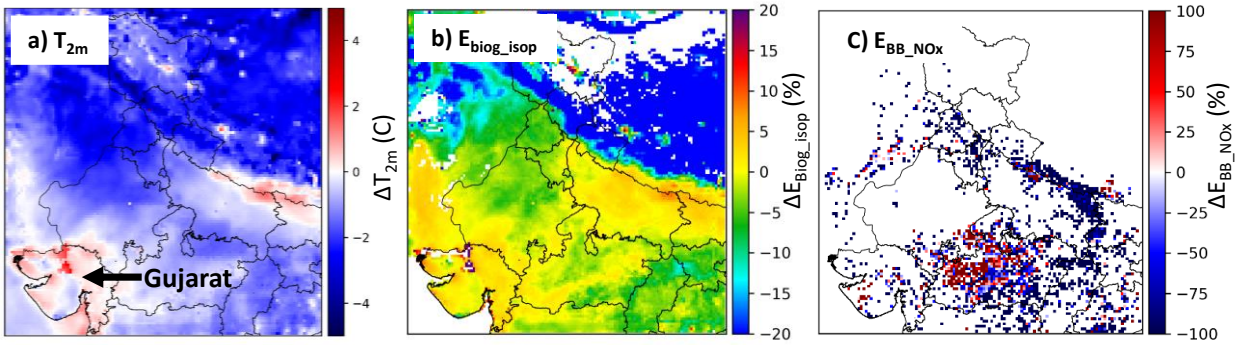

Figure 5 Difference between April 2020 and 2019 in modeled daytime averaged a) 2-m temperature, b) biogenic isoprene, and c) biomass burning NOx emissions over the domain

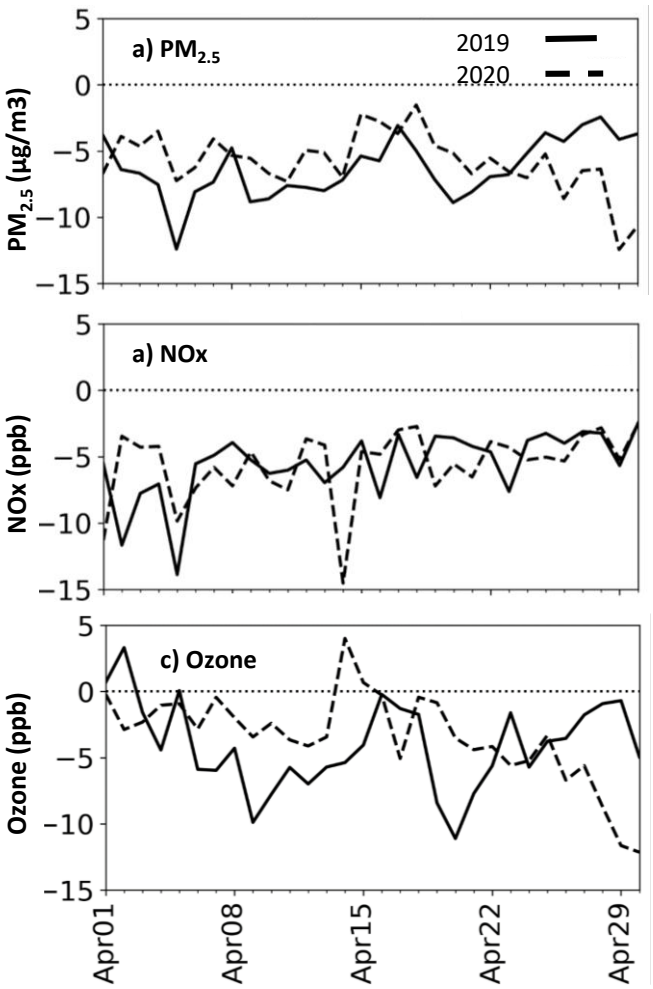

Figure 6 Effect of lockdown emissions on daytime a) $PM_{2.5}$, b) NOx, and c) Ozone concentration in April 2019 (solid line; difference between 2019COVID and 2019BAU) and 2020 (dashed line; difference between 2020COVID and 2020BAU).

In order to attribute the changes between April 2019 and 2020, we looked at three scenarios. The difference between 2020BAU and 2019BAU indicates the effects of meteorology, while the difference between 2020COVID and 2020BAU presents the effects of lockdown emissions. Figure 7 and Figure 8 show the percentage of point-to-point changes due to meteorology, emissions, and their combined effects (the difference between 2020COVID and 2019BAU) on averaged daytime concentrations in April. In the following analysis, we focus only on India and disregard the changes over the boundaries (affected majorly by IC/BC) and over Himalayan region (very low concentrations). Similar plots for the IGP region is provided in the supporting information (Figure S6 and Figure S7).

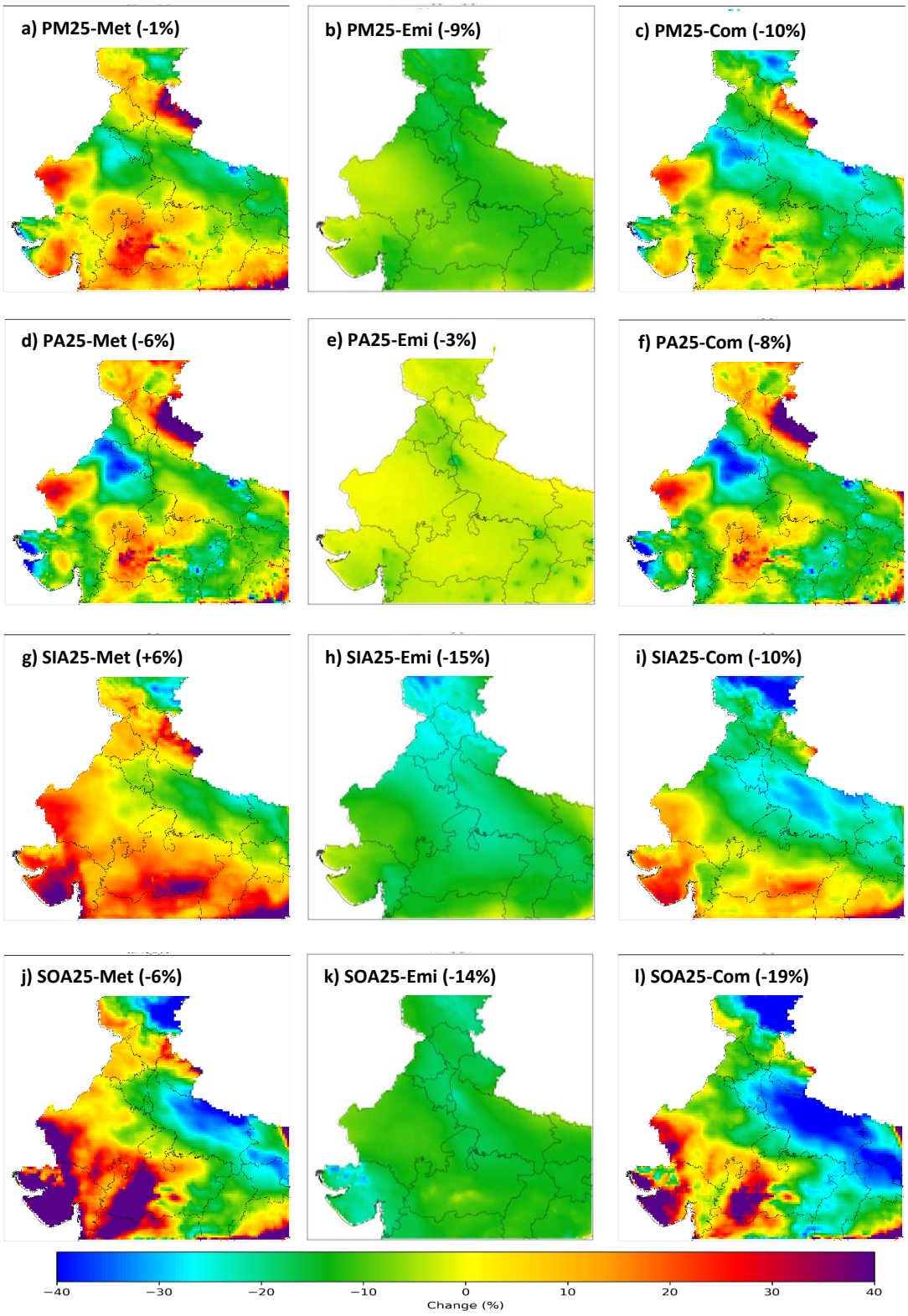

Figure 7 Responses of April averaged daytime $PM_{2.5}$ (first row), $PA_{2.5}$ (second row), $SIA_{2.5}$ (third row), and $SOA_{2.5}$ (fourth row) concentrations to meteorology (left column), emission (middle column), and combined (right column) effects. The numbers in the parenthesis show the averaged change over the colored region between April 2020 and 2019.

The averaged daytime $PM_{2.5}$ concentrations in April in India decreased by only one percent due to the meteorology effects. However, each region in the domain showed different changes. Figure 7 shows that larger $PM_{2.5}$ concentration reductions over the IGP due to the meteorology effects (Figure S6 shows 06% for the IGP). The reduction was more intense in some parts of the IGP, e.g. west of Delhi (~25%). It also shows $PM_{2.5}$ concentrations increased over central India by more than 40% over the regions mostly affected by biomass burning emissions. On the other hand, the lockdown emissions decreased $PM_{2.5}$ concentrations almost everywhere in India (i.e. the IGP and central India) with the average of 9% and the maximum of ~20% in Delhi. The combined effects show a large reduction in $PM_{2.5}$ concentrations over the IGP (by up to 35%). However, the increase due to the meteorology over central India offset the decrease due to the lockdown emissions. The changes in $PM_{2.5}$ composition as primary aerosols ($PA_{2.5}$; sum of organic carbon, black carbon, and primary inorganics), secondary inorganic aerosols ($SIA_{2.5}$; sum of nitrate, sulfate, and ammonium), and secondary organic aerosols ($SOA_{2.5}$) are also shown. All $PM_{2.5}$ constituents showed a reduction over eastern IGP and an increase over central India due to the meteorology. The amount of changes were larger for $SOA_{2.5}$ both in the eastern IGP and central India, suggesting biomass burning emissions had larger impacts on SOAs. However $PA_{2.5}$ decreased by up to 40% in the western IGP, while $SOA_{2.5}$ and $SIA_{2.5}$ changed by less than 10%. The large primary inorganics component of $PA_{2.5}$ and faster wind speeds on the border of India and Pakistan suggest that dust emissions affected this region in April 2019 (Figure S8). Other studies have also reported pre-monsoon windblown dusts over western India (R. Kumar et al., 2014; Sarkar et al., 2019). Lockdown emissions decreased $SIA_{2.5}$ and $SOA_{2.5}$ between ~10-25% over the IGP with large changes over Delhi (~25%). Similarly, $PA_{2.5}$ decreased by ~10% over Delhi and surrounding areas. Similar reductions can be seen on some other urban areas over the domain. However, lockdown emissions did not change $PA_{2.5}$ very much (<10%) in non-urban areas as AFs for BC in India (Figure 2) suggested. Furthermore, solid fuels are the primary source of cooking and heating in non-urban regions in India and it did not change during the lockdown period (Beig et al., 2021). The combined effects show larger impacts of meteorology on $PA_{2.5}$ and $SOA_{2.5}$ in the IGP, while changes in emissions due to lockdown had larger impacts on $SIA_{2.5}$ (Figure S6).

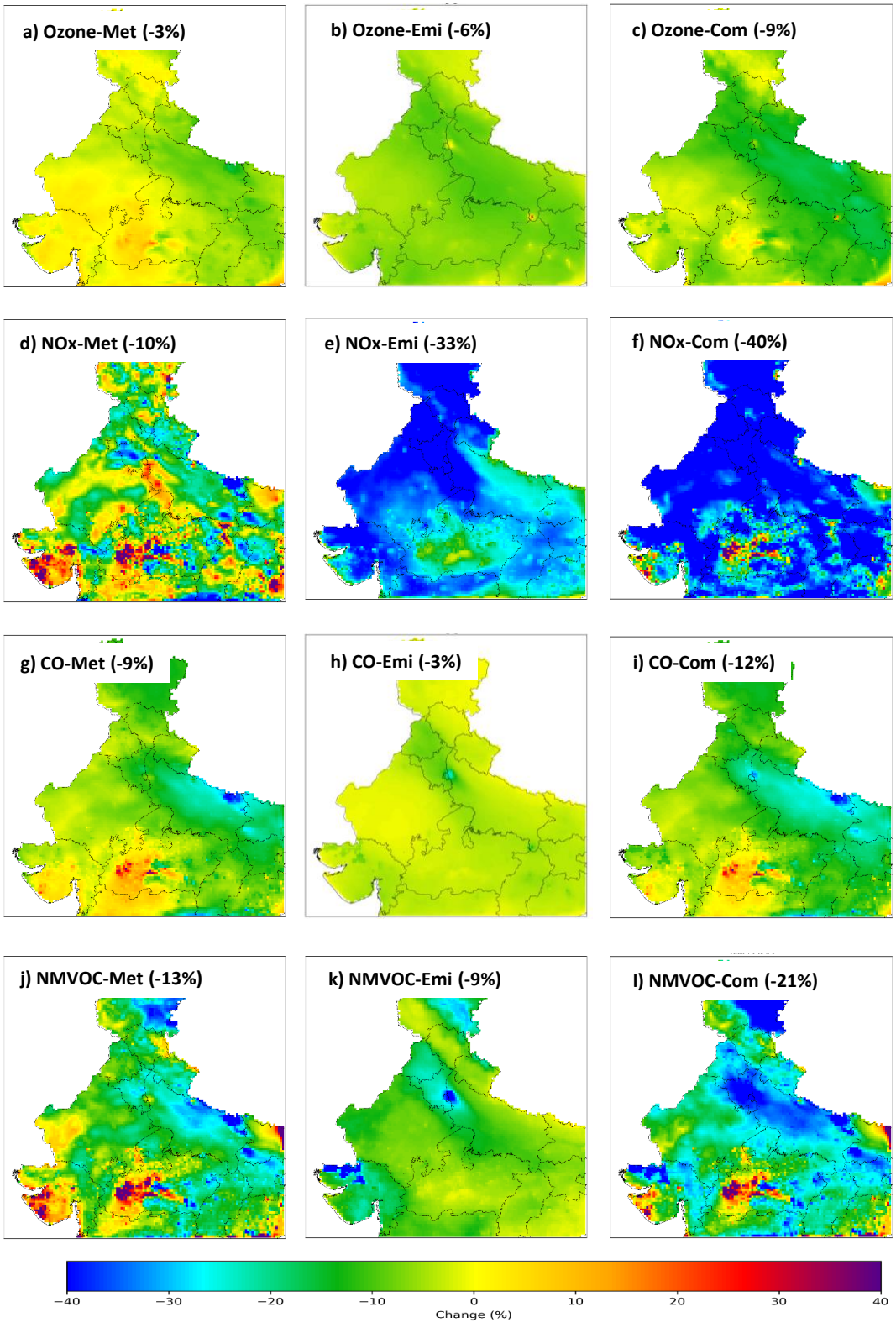

Figure 8 Responses of April averaged daytime ozone (first row), NOx (second row), CO (third row), and NMVOC (fourth row) concentrations to meteorology (left column), emission (middle column), and combined (right column) effects. The numbers in the parenthesis show the averaged change over the colored region between April 2020 and 2019.

In general, the effects of meteorology on ozone was similar to $PM_{2.5}$. Figure 8 shows that meteorology effects led to lower (up to -20%) and higher (up to 20%) daytime ozone mixing ratios over the IGP and central India, respectively. Regarding the ozone precursors, emission effects was significant for NO_x concentration (-33%). Largely the changes in ozone can be explained by the changes in NOx, as for most parts of the domain ozone is NOx-limited (as will be discussed in Section 3.2). For example, the changes in NOx emissions due to the lockdown are large and rather uniform over the domain. Throughout most of the domain, NOx concentrations due to emission perturbations decreased by over 30%. The ozone decreases are strongly correlated with the regions with large NOx decreases. We can see only the major cities like Delhi and the regions with many power plants experienced increases in ozone mixing ratio with decreases in NOx emissions. On the other hand, ozone mixing ratio (combined effect) in the southern parts of the domain increased although lockdown emissions reduced NOx concentration. This is a region where the NOx concentrations increased due to meteorology (as shown in the change in NOx-Met subplot), which was due to the larger biomass burning emissions in April 2020 as shown in Figure 5. The net effect is that NOx concentrations increased in this region and this lead to higher ozone concentrations. The meteorology effect on NMVOCs and CO concentrations shows lower concentrations over the IGP and higher concentrations in central India in April 2020. While biogenic emissions were higher in the IGP in April 2020, lower biomass burning emissions (as shown in Figure 5) explain the meteorology effects on NMVOCs and CO concentrations in this region. Emission perturbations decreased NMVOCs concentrations over India on average by 9%, while the reduction was ~40% in Delhi (similar to NO_x). The effect of emissions on CO concentration was small over India (averaged reduction of 3%). This magnitude was larger in Delhi (~25% reduction) and in lower magnitudes in other parts of the IGP. The combined effects of meteorology and lockdown emissions on ozone and its precursors showed reduction in daytime concentrations over all parts of India except central India. In central India, both biogenic emissions and biomass burning emissions were higher in April 2020.

To better illustrate the response of ozone to changes in NOx and NMVOC concentrations, we show the response of the model in all the grid cells in Delhi (i.e. Urban) to the lockdown emission changes during all daytime hours in April (Figure 9). In Delhi, daytime NMVOC concentrations decreased up to 60% and NO_x concentrations decreased up to 70%. Ozone concentration showed both decreasing and increasing response to the precursor reductions. Ozone increased in 20% of grid cells. In addition, most of these increasing ozone data points belong to four (out of 20) grid cells located in the eastern part of the Urban subdomain (not shown). It is important as local emission inventories also show Delhi (i.e. Urban) is most densely populated in its eastern border. The largest increases were observed at NMVOC and NO_x reductions of more than 40%. Power and Rural showed lower reductions in the precursor concentrations and only a small number of grid cells showed an increased ozone response (Figure S9).

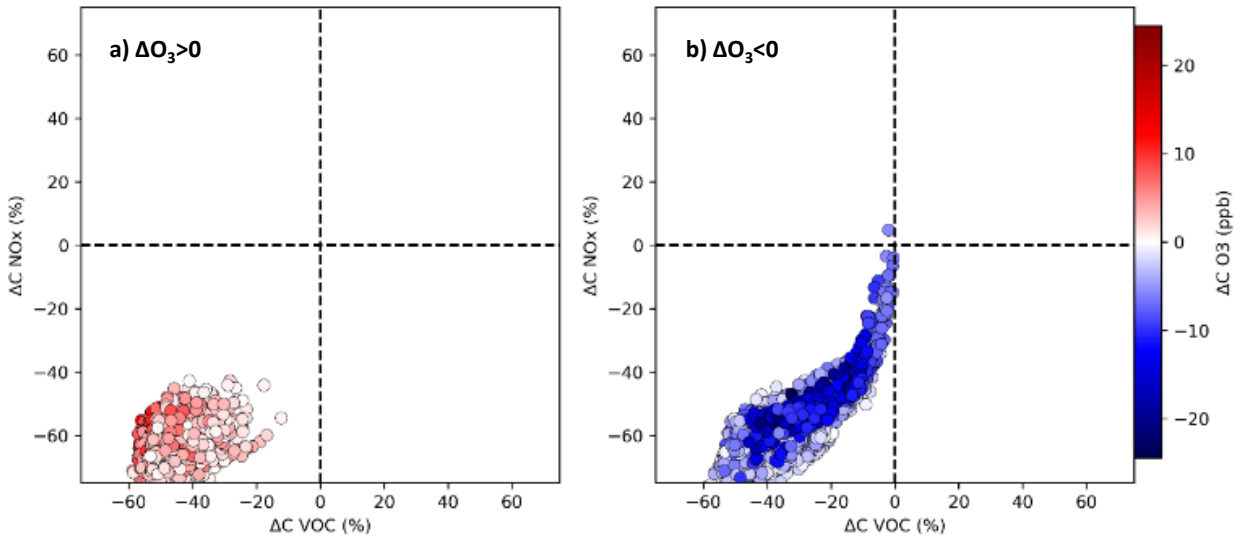

Figure 9 Plot of changes in NOx (Y-axis) and NMVOC (X-axis) concentrations due to the lockdown (2020COVID – 2020BAU) and ozone a) increasing and b) decreasing responses in all the grid cells within the Urban region (20 grid cells) during April (30 days) daytime (1000-1700 LT) hours (total data points are 4800). X- and Y-axis are normalized values. 5th layer in the model was selected to minimize the impacts of direct emissions.

3.2. Process Analysis of ozone chemistry

As presented in the previous section, the changes in ozone concentrations did not exactly follow the changes in its precursors' emissions during the lockdown period. Specifically, NO_x and VOCs anthropogenic emissions were significantly decreased as a response to lockdown in India by up to 40% (Figure 2), whereas daytime ozone concentrations showed only a 6% reduction (Figure 8). More interestingly, 24-hour averaged ozone mixing ratios were higher on some days over Delhi during the lockdown period compared with the pre-lockdown period (Figure S5). In this section, we utilize the IRR capability of WRF-Chem to study the chemistry of ozone. We chose two sample days representing pre-lockdown and lockdown conditions to look at the ozone chemistry in previously-defined Urban, Power, and Rural regions. In order to choose these two days, we applied a meteorological filter in Urban to select the days with the most similar meteorology between years 2019 and 2020. We calculated the daytime averaged 10-meter wind speed and 2-meter temperature for each day in both years and found the day with lowest overall normalized biases (Figure S10). As a result, 13 March and 7 April were selected as the sample pre-lockdown and lockdown days, respectively. Nevertheless, it is important that these days were selected based on the filters in Urban and did not necessarily represented lowest-meteorological-variability days in Power and Rural (Figure S10). As an experiment, we applied the same methodology over India and found two other days with the least variability over the domain. However, it did not majorly affect the following analysis (not shown). We acknowledge that this technique of choosing the days does not consider the effects of previous days.

It is important to understand the general processes in the ozone chemistry; we provide a simplified overview of the complex chemistry of ozone in the troposphere. While NO_x and VOCs (including CO, and methane (CH_4)) are the main precursors of ozone, hydroxyl (OH) radical is also a key species in the ozone chemistry. The reason is that OH can oxide VOCs and produce organic proxy radicals (RO_2) as shown in Eq1. Then, RO_2 can react with NO and produce NO_2 without involving ozone (Eq2: for simplicity, we do not show the pathway towards hydroperoxyl radical (HO_2) formation), which can

eventually lead to net ozone via Eq3 and Eq4. On the other hand, the ozone photolysis is the main source of tropospheric OH. Thus, this loop (Eq1 to Eq4) continues to form ozone during daytime (*hv*) as far as VOCs and OH are available in the atmosphere (NOx acts more as a catalyst in this loop). Relative to VOCs, CO and CH_4 react very slowly with OH. Thus, short-lived VOCs become important as their availability primarily depend on their emissions. However, we should emphasize that it does not necessarily mean that large amounts of VOCs will increase ozone (i.e. radical loss via radicals (LRO_x)). In terms of OH, it can also react with NO_2 and form nitric acid (HNO_3), and remove both OH (and other radicals) and NO_2 (Eq5; this is the main reaction of radical loss via NOx termination (LNO_x)). In other words, VOCs reactivity with OH (VOC+OH) shows a path to ozone formation (Eq1), and NO_2 reactivity with OH (NO_2+OH) presents an obstacle to ozone formation (Eq5). During nighttime, photolysis of NO_2 (Eq3) does not occur, halting ozone formation cycle; rather, NO_2 reacts with ozone and form gas phase radical nitrate (NO_3) through Eq6. Moreover, available NO consumes ozone and produces NO_2 (Eq7), accelerating NO_3 chemistry, resulting in net ozone destruction. More detailed chemistry of ozone can be found elsewhere (e.g. Pusede and Cohen (2012); Seinfeld and Pandis (2016))

$$VOC + OH \xrightarrow{O_2} RO_2 + H_2O \quad \text{Eq1}$$

$$RO_2 + NO \rightarrow RO + NO_2 \quad \text{Eq2}$$

$$NO_2 + hv \rightarrow NO + O \quad \text{Eq3}$$

$$O + O_2 \xrightarrow{M} O_3 \quad \text{Eq4}$$

$$OH + NO_2 \xrightarrow{M} HNO_3 \quad \text{Eq5}$$

$$NO_2 + O_3 \rightarrow NO_3 + O_2 \quad \text{Eq6}$$

$$NO + O_3 \rightarrow NO_2 + O_2 \quad \text{Eq7}$$

Figure 10 shows the surface ozone mixing ratio and planetary boundary layer height (PBLH) averaged within Urban, Power, and Rural regions for a pre-lockdown (13 March) and lockdown (7 April) days. First, we analyze the pre-lockdown day in Figure 10 (left column). It shows the differences within each region was only because of meteorology (2019 vs 2020). In Urban, the evolution of planetary boundary layer (PBL) was similar for both 2019 and 2020 scenarios and ozone followed similar trend as the PBL, with the peak at 1530 LT. In Power, the PBLH was lower in 2020 (1km) compared with 2019 (3km), which is consistent with this day's lower temperature and higher wind speed in 2020 (Figure S10). However, ozone mixing ratio were close to each other although peaked at different hours (1530 LT in 2019 vs 1130 LT in 2020). Similarly in rural, models showed different PBL evolution, while ozone mixing ratio showed a smooth similar pattern between 2019 and 2020.

Second, we analyze the lockdown day (7 April) in Figure 10 (right column). In Delhi, the PBL grew faster and extended higher in 2020, while both years peaked during afternoon hours. The shallower PBLH in 2019 means more precursors are available in the shallower atmosphere (i.e. less dilution), leading to more ozone formation during the day. Moreover, the model simulated higher CO concentrations over the IGP in 2019 (not shown). Srinivas et al. (2016) found that transported pollution from the Bay of Bengal can potentially elevate the CO concentrations in Delhi. We are also interested in the impacts of lockdown emission. Comparing 2020BAU and 2020COVID, the lockdown resulted in lower peak value. It should be emphasized that this was not the case for the all days during the lockdown period as the impact of emissions on daytime ozone mixing ratio varied day by day in Urban (Figure 6). On the other hand, the

largest difference in ozone mixing ratio happens during 0030-0730 LT and 1830-2330 LT. While the reaction between NO and ozone should deplete all the ozone in the atmosphere, the titration did not deplete all the ozone in 2020COVID scenario due to lower amounts of NO available. As a result, some residual ozone remained in the atmosphere.

In Power, the PBL grew faster in 2020 but its peak height was lower than 2019. However, the daytime ozone mixing ratios did not change between both years (although the morning time (0830-1030 LT) ozone was higher in 2019 due to lower PBLH). We also observed small changes between 2020BAU and 2020COVID scenarios. Although the percentage of emission changes were large for both VOCs and NOx, the amount of anthropogenic VOC emissions were low in this region and NOx emissions in Power were even more than Urban (Table S3). Furthermore, the eastern IGP was also significantly impacted by biogenic emissions in 7 April 2020 (Figure S11). As a result, biogenic VOC emissions controlled the ozone formation, which were similar in both 2020BAU and 2020COVID scenarios.

In Rural, the PBL growth in 2019 was faster and it extended higher than 2020. Figure S10 also shows that wind speed in Rural was lower by ~75% on 7 April 2020 compared with the same day in 2019, leaning towards a stagnant condition. As a result, the ozone mixing ratio is higher in 2020 scenarios. Comparing 2020BAU and 2020COVID shows a reduction during all hours due to the lockdown emissions.

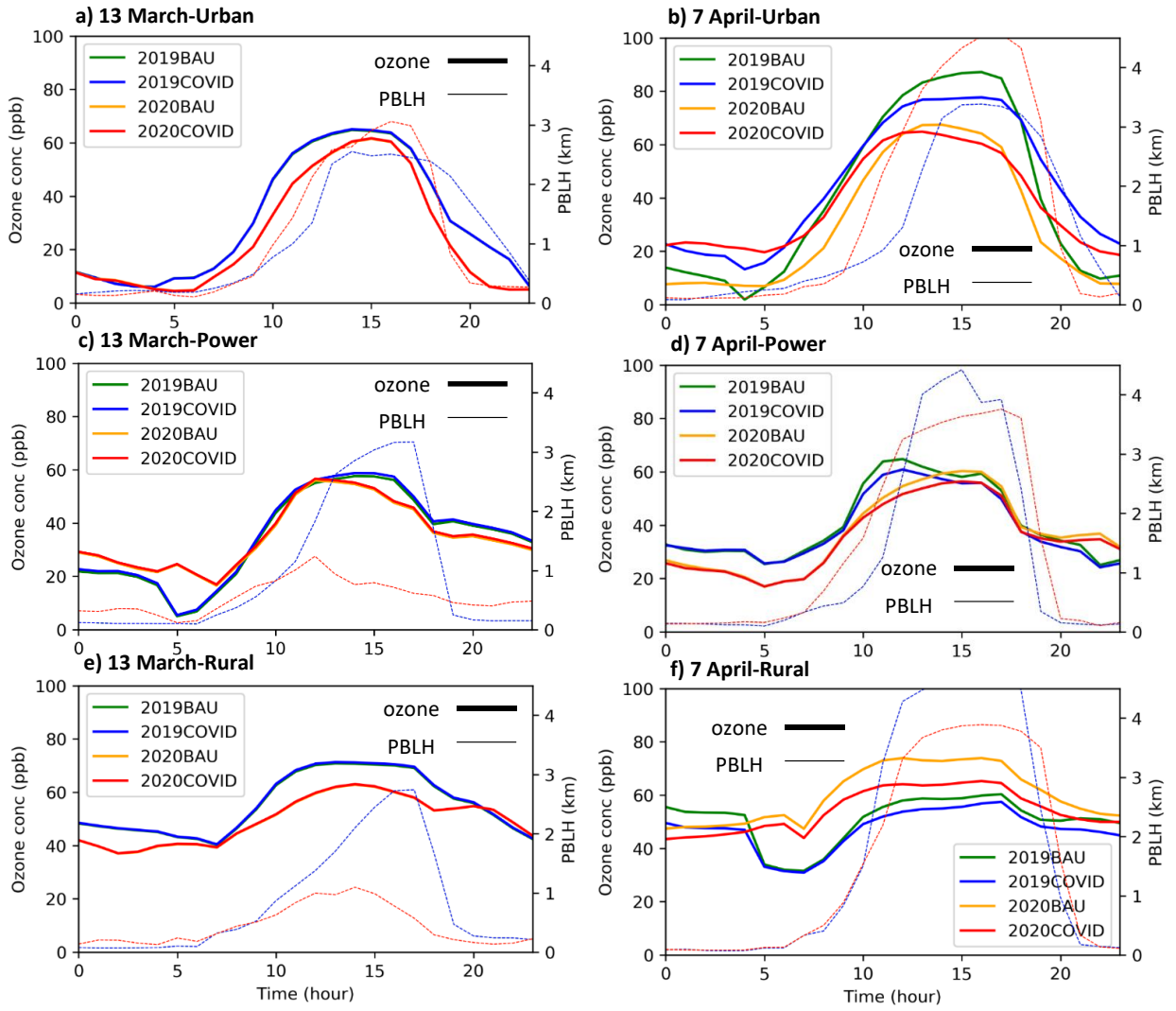

Figure 10 Surface ozone mixing ratio (primary Y-axis) and PBLH (secondary Y-axis) averaged over Urban (top row), Power (middle row), and Rural (bottom row) for a sampled pre-lockdown day (13 March: left column) and lockdown day (7 April: right column).

Figure 11 shows the OH reactivity with VOCs and NO_2 within Urban, Power, and Rural regions for a pre-lockdown (13 March) and lockdown (7 April) day. We followed Pfister et al. (2019) suggestion in averaging these values within the PBL to minimize the effects of mixing. It is important to note (1) these OH reactivity plots are averaged within the PBL, while ozone mixing ratios in Figure 10 were surface values and (2) these plots indicate the chemistry contribution to the ozone mixing ratio, while other contributing factors such as vertical mixing and advection are also important processes impacting the actual ozone mixing ratio (Pusede & Cohen, 2012).

During the pre-lockdown day, VOC+OH and NO2+OH were different for 2019 and 2020 in Urban. Although there were also some differences in the time of the peaks, the ratio of VOC+OH to NO2+OH was similar, suggesting the ozone formation was not very much different. In Power, the VOC+OH increased in 2020, while the peak of NO2+OH did not change. It shows that meteorology effects (including natural sources emissions) majorly affected OH reactivity with VOC in Power. In Rural, the

results showed smaller VOC+OH rates in 2020 with roughly similar NO2+OH rates. However, both VOC and NOx anthropogenic emissions were low in this region and very similar between 2019 and 2020. Similarly, it indicates the importance of meteorology effects and accompanied biogenic and biomass burning emissions on the ozone formation in Rural.

During the lockdown day, OH reactivity (with both VOC and NO_2) was higher in 2019 scenarios than 2020 in Urban. This is consistent with shallower PBL in 2019, which led to higher ozone mixing ratios. In 2020 scenarios, the NO2+OH rate dropped in 2020COVID compared with 2020BAU (0.5 ppb/hr), with smaller reductions in VOC+OH rate (0.2 ppb/hr). Until 1230 LT, the model did not show any large reductions in VOC+OH (i.e. ozone formation did not change), while NO2+OH showed large drops (i.e. ozone destruction decreased). Similarly, we saw larger surface ozone mixing ratios until noon in 2020COVID scenario. After 1230 LT, the VOC+OH showed larger reductions, leading to lower net ozone formation in the 2020COVID scenario.

In Power, larger OH reactivity values were observed for both VOC and NO_2 in 2019 compared with 2020. This was unexpected as we observed larger biogenic isoprene emissions in 7 April 2020 (Figure S11). However, it can be explained by higher CO contribution in 2019 results (Figure S12). On the other hand, the biogenic soil NO emission was also larger in 2019; resulting in more ozone formation. Considering the lockdown emissions, the model showed that adjusted emissions (i.e. COVID scenarios) did not change VOC+OH values. This is due to low anthropogenic and equal biogenic VOC emissions in this region. NO2+OH values decreased as NOx emissions reduced

In Rural, we observed similar behavior of OH reactivity for both 2019 and 2020. It is consistent with similar ozone mixing ratio trend in Figure 10. As emissions are low in this region, ozone formation and OH reactivity does not play an important role and ozone differences can be explained by dynamics and atmospheric stability. As a result, adjusted emissions had similar effect on both VOC+OH and NO2+OH rates in 2020 scenarios.

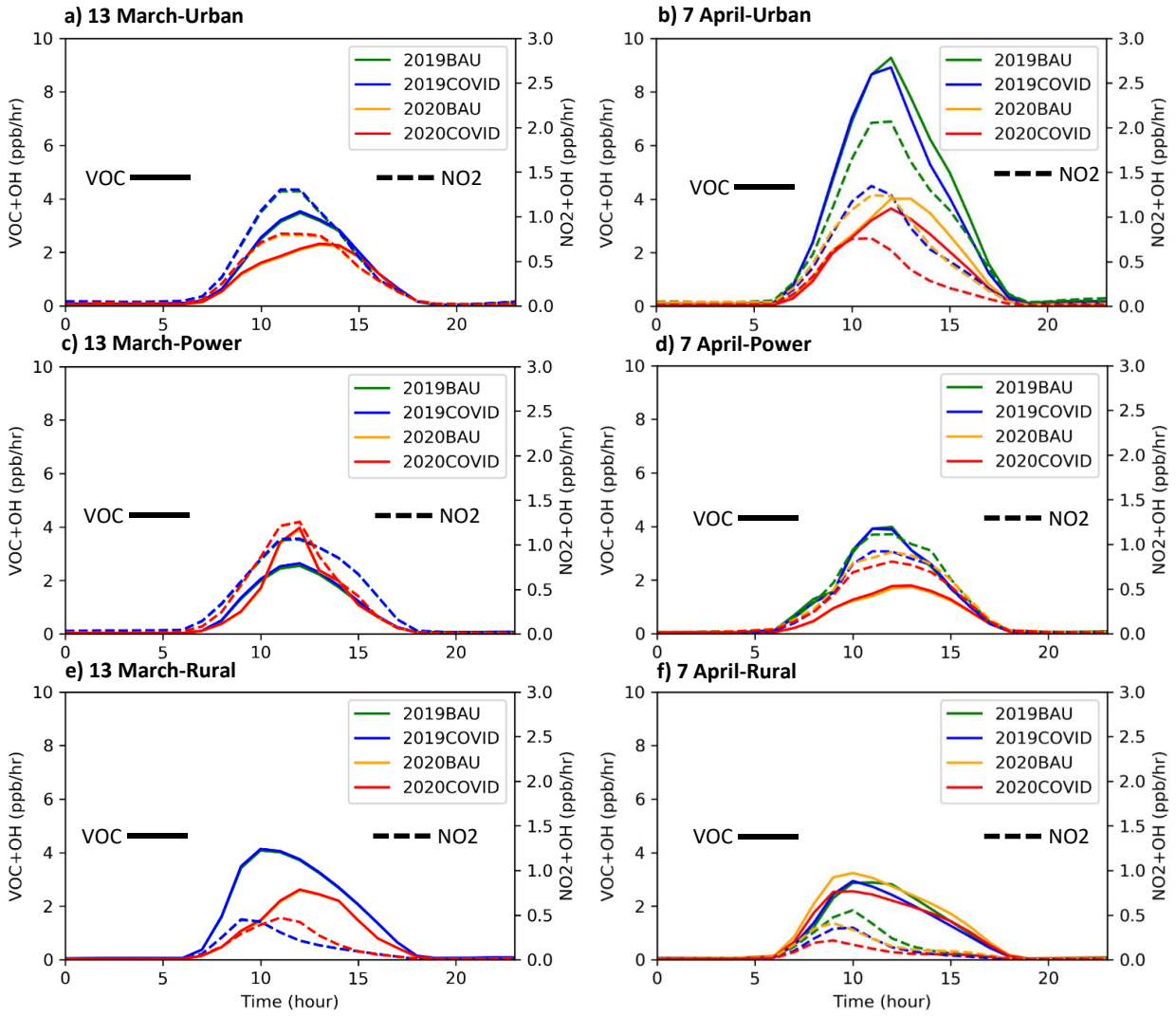

Figure 11 OH reactivity with VOCs (primary Y-axis) and NO2 (secondary Y-axis) averaged within PBL over Urban (top row), Power (middle row), and Rural (bottom row) for a sampled pre-lockdown day (13 March: left column) and lockdown day (7 April: right column).

Since there are many VOCs available in the atmosphere, IRR gives us the opportunity to find the species that have higher contributions to the OH reactivity. Figure S12 shows the OH reactivity for the top six VOC species for the lockdown day in each region and scenario. CO was the main component in all the regions and scenarios. Although CO reacts slowly in the atmosphere (i.e. long lifetime), its abundant availability moves it to the top of the list. The other species were short-lived species. Formaldehyde (CH2O) was the second-ranked species in almost all the subfigures except the ones that isoprene (ISOP) had more reactivity rate. Specifically, ISOP was the second-ranked species in Power region in all the scenarios. This is because VOCs in Power region were dominated with biogenic sources and changing the anthropogenic emissions did not change their rankings. Regardless, the meteorology affected the magnitude of the contribution between the two years. ISOP was also the second-ranked species in Urban in 2020COVID scenario. High contributions by CO and CH2O to OH reactivity is also reported in the United States (Pfister et al., 2019). They found that high contribution of CH2O to OH reactivity was due

to both local emissions and chemical production, while ISOP was mostly due to biogenic emissions. While CH2O had larger contribution in the Urban, ISOP had larger contributions in the Power, which is consistent with Pfister et al. (2019). In Urban, the transportation sector had the largest contribution in anthropogenic emissions of CH2O (~90%) and residential sector had about 10% of its emission. We also found contributions from the large alkenes (BIGENE), which is a tracer of anthropogenic VOCs, in BAU scenarios in Power. Comparing the ranking of ISOP in 2020BAU and 2020COVID for Urban shows biogenic emissions had a larger contribution during the lockdown. It points to the need to consider the background biogenic emissions when evaluating expected changes in ozone due to anthropogenic emissions reductions. Large alkanes (BIGALK) contributed to the OH reactivity over Urban in 2019BAU and 2020BAU and over Rural in 2020BAU. BIGALK is another tracer of anthropogenic VOCs, and its contribution in Rural indicates the impact of transport on ozone mixing ratio in this region. Analysis of the HTAP emission inventory revealed that the transportation sector has the largest BIGALK and BIGENE emissions in Urban (~90%). The second-ranked anthropogenic sector in Urban was the industrial sector for BIGALK emission and residential sector for BIGENE emission. When looking at the entire domain (i.e. India region), transportation sector had the largest BIGALK emission, while the residential sector had the largest contribution for BIGENE and CH2O emission.

As discussed earlier, LROx and LNOx are the reactions that determine the radical terminations by radicals and NOx, respectively, during the daytime (Table S6 and Table S7). More information on IRR analysis methodology is provided in the supporting information. The LROx/LNOx ratio is very important from policy's perspective as it indicates whether reduction in NOx (large ratio values; i.e. NOx-limited) or VOCs (small ratio values; i.e. VOC-limited) emission is the efficient strategy for ozone reduction. Duncan et al. (2010) assumed the transition between NOx-limited and VOC-limited regions happens at a LROx/LNOx ratio of one. Schroeder et al. (2017) found the transition of ozone production occurs at a ratio of 0.35 using 0-D photochemical box modeling. However, evaluating the LROx and LNOx values is not usually possible based on observations. As a result Sillman (1995) proposed using the ratio of measured tracers in the atmosphere as an alternative. The formaldehyde to NO_2 ratio (FNR) is one of the most frequently used ratio as its species can be measured from both ground measurements and space borne instruments (Jin & Holloway, 2015; V. Kumar et al., 2020; Martin et al., 2004). Mahajan et al. (2015) used the FNR transition range between one and two to study the inter-annual variations of ozone formation in India using satellite observations, whereas Schroeder et al. (2017) showed this transition range is not constant in all regions. For example, they found in their box modeling study in the US that the transition range was 0.9-1.80 in Colorado, while the range of 0.7-2.0 was found for Houston, Texas. In other words, the FNR transition range for each region should be exclusively specified for each region.

Figure 12 shows the plots of FNR ratio within the PBL as a function of LROx/LNOx in Urban, Power, and Rural for the 2019BAU and 2020BAU scenarios during the afternoon hours (1230-1430 LT). The results for 2019BAU (2020BAU) show that 65% (67%) of points were in the VOC-limited region (i.e. LROx/LNOx<0.35) in Delhi, whereas only 1% (2%) of the points were in the VOC-limited region in Rural. These results show that ozone formation regime differs for each region and indicate that we cannot employ one uniform emission control strategy everywhere in the IGP (and India). The results for Delhi support the idea that the emission control strategies that target the transportation sector, with the primary goal of PM reduction, can increase ozone (Chen et al., 2020). In Power, 64% (65% for 2020BAU) of the data-points were in the VOC-limited region, which is expected as this domain had low amounts of anthropogenic VOCs emissions (Table S3) and biogenic emissions were the primary source VOCs (Figure S12), suggesting extreme NOx emission reduction may be the only solution in this region. While the effect of different meteorology (2019BAU vs 2020BAU) on chemical regimes were negligible, dramatic changes in emissions can lead to large changes. For example, only 34% of points were in the

VOC-limited regime in Urban for 2020COVID scenario, in which both NMVOC and NOx emissions had large reductions (Figure S13).

Calculating binned averages and corresponding standard deviations for the FNR data can provide some insights about the transition range (Schroeder et al., 2017). We also took the union of the transition range of 2019BAU and 2020BAU scenarios to minimize the effect of meteorology. In Urban, our results suggest that the FNR transition range is 0.4-1.1. However, it is clear that this range covers a large amount of data points in other bins as well. In Power, the lower range of the transition range goes to zero due to the large amounts of NOx emissions in this region. However, the upper range (1.2) can be used as a cut-off between VOC- and NOx-limited regimes in Power. In Rural, the transition range is 0.7-1.3, which was derived based on less than 5% of the data. We also observed larger LROx/LNOx ratios in Rural compared with other regions, indicating the role of biogenic emissions in non-urban regions. Schroeder et al. (2017) emphasized that other parameters (e.g. different radicals with different lifetimes than formaldehyde) can affect the FNR ratio and it may not be a solid indicator of ozone formation sensitivity in some regions. Furthermore, Souri et al. (2020) studied the functionality of FNR ratio and found situations where LROx/LNOx and FNR lead to contradicting conclusions regarding the chemical regime in a region, primarily because of impacts of NO_2 on formaldehyde.

Figure 13 shows the FNR ratio using 2020BAU and 2020COVID scenarios averaged in Urban, Power, and Rural during afternoon hours (1230-1430 LT) in April 2020. In Urban, 29 days were estimated to be in the transition range in 2020BAU scenario, while they were mostly close to the lower limit of the transition range (i.e. toward VOC-limited). Applying the lockdown emissions increased the FNR ratio by an average value of 0.48 and shifted almost all the days into either a NOx-limited or an upper limit of the transition range. Although it slightly changed the ozone formation regime, we did not see any major change in daytime ozone concentration in Urban (Figure S14). In Power using 2020BAU scenario, we observed that only four days in April were completely in a NOx-limited regime while the FNR in rest of the days were lower than the upper-limit of the transition region. The FNR ratio increased by an average value of 0.21 because of lockdown emissions reductions (i.e. 2020COVID). However, about half of the days remained below the upper-limit of the transition and did not moved to NOx-limited region, showing the lockdown emissions did not majorly change the ozone formation chemistry in Power. In Rural, almost all the days (28 days) were already in the NOx-limited regime in 2020BAU scenario. As a result, increasing the FNR ratio by an average value of 0.49 due to the lockdown emissions (i.e. 2020COVID) did not change the ozone formation chemistry in Rural.

Using the upper-limit of the calculated transition regime (1.3) in the three mentioned regions, we looked at the ozone production regimes for the entire study domain (Figure 14). We found that most parts of India are in the NOx-limited regime. Indeed, all the regions except the urban areas, power plant region, and western IGP fall in the NOx-limited regime. The FNR in Haryana state was lower than 1.3, showing the state is in the VOC-limited regime. There are some locations in Punjab state with VOC-limited regime (FNR<1.3), while other locations are slightly in NOx-limited regime. Likewise, there are some locations (cities) in Uttar Pradesh with FNR close to 1.3 (i.e. close to VOC-limited regime). Using the lockdown emissions (2020COVID), the FNR increased over the domain, moving most parts of the Punjab and Haryana states into NOx-limited regime. On the other hand, the FNR in some urban locations (e.g. Delhi) and the Power region remained below 1.3; the ozone production regime did not change. Overall, our analysis indicate that the FNR can determine a region that is strictly NO_X- or VOC-limited (e.g. Power and Rural) but caution should be exercised for regions close to the defined transition regions (e.g. Urban).

Comparing the total OH consumed by each pathway (i.e. integrating the 24-hr values in Figure 11 for 7 April as the lockdown day) and their ratio in 2020BAU and 2020COVID scenarios can also provide some

information on whether ozone chemistry regime changed because of the lockdown. Table S8 shows integrated values in total OH consumption by VOCs was higher in Urban and Rural compared with Power, confirming low VOCs in Power region. Moreover, the ratio of total OH consumption by VOC to NO_2 had smallest values in Power, showing the preference of NO_2+OH pathway in this region. Evaluating the change of the ratio because of lockdown emissions indicates that Urban and Rural shifted toward NOx limited regime, while the ozone chemistry regime did not change in Power.

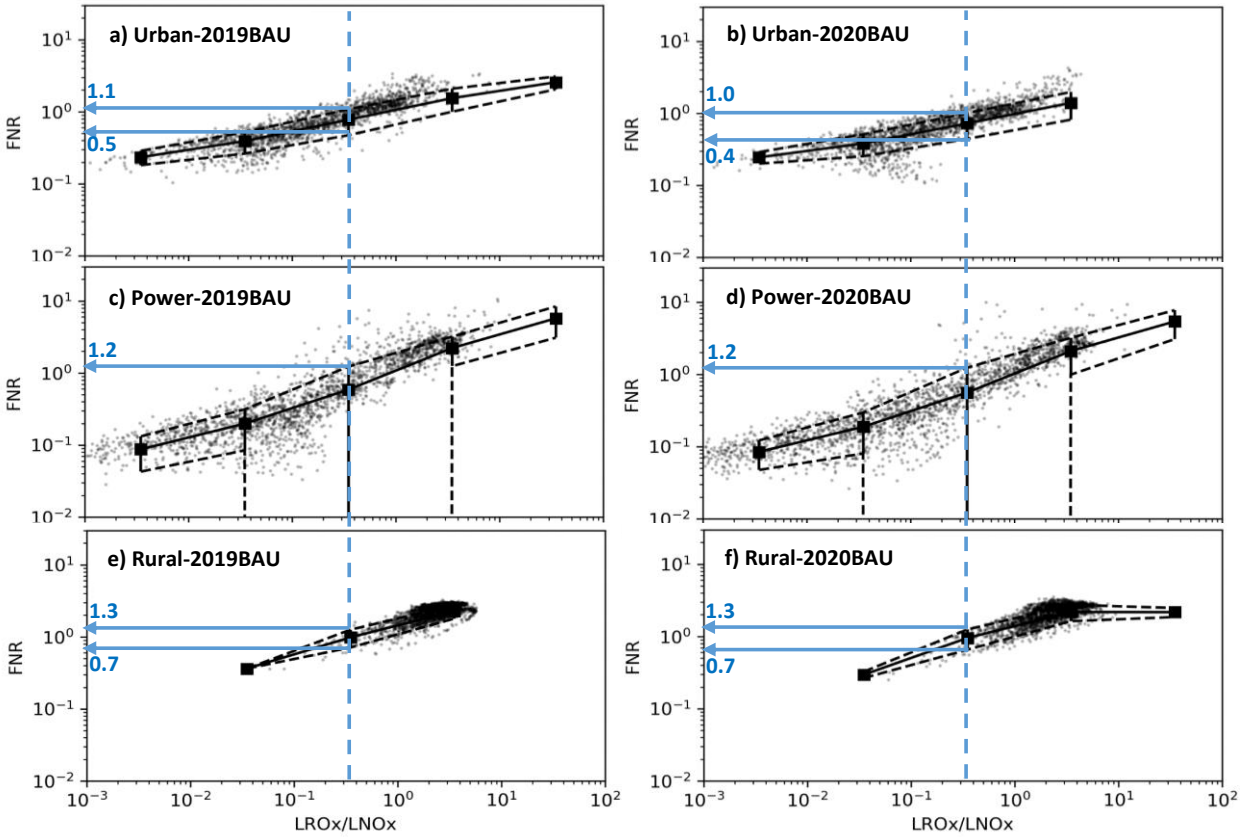

Figure 12 Plots of point-to-point FNR ratio (within the PBL) as a function of LROx/LNOx ratio during afternoon hours (1230-1430 LT) for 2019BAU (left column) and 2020BAU (right column) scenarios in a, b) Urban, c, d) Power, and e, f) Rural regions. Binned averages (black squares) and standard deviations (vertical black bars) were calculated. The vertical dashed blue line represents LROx/LNOx ratio of 0.35. The horizontal blue vectors show the FNR transition range in each region (numbers in blue show the values).

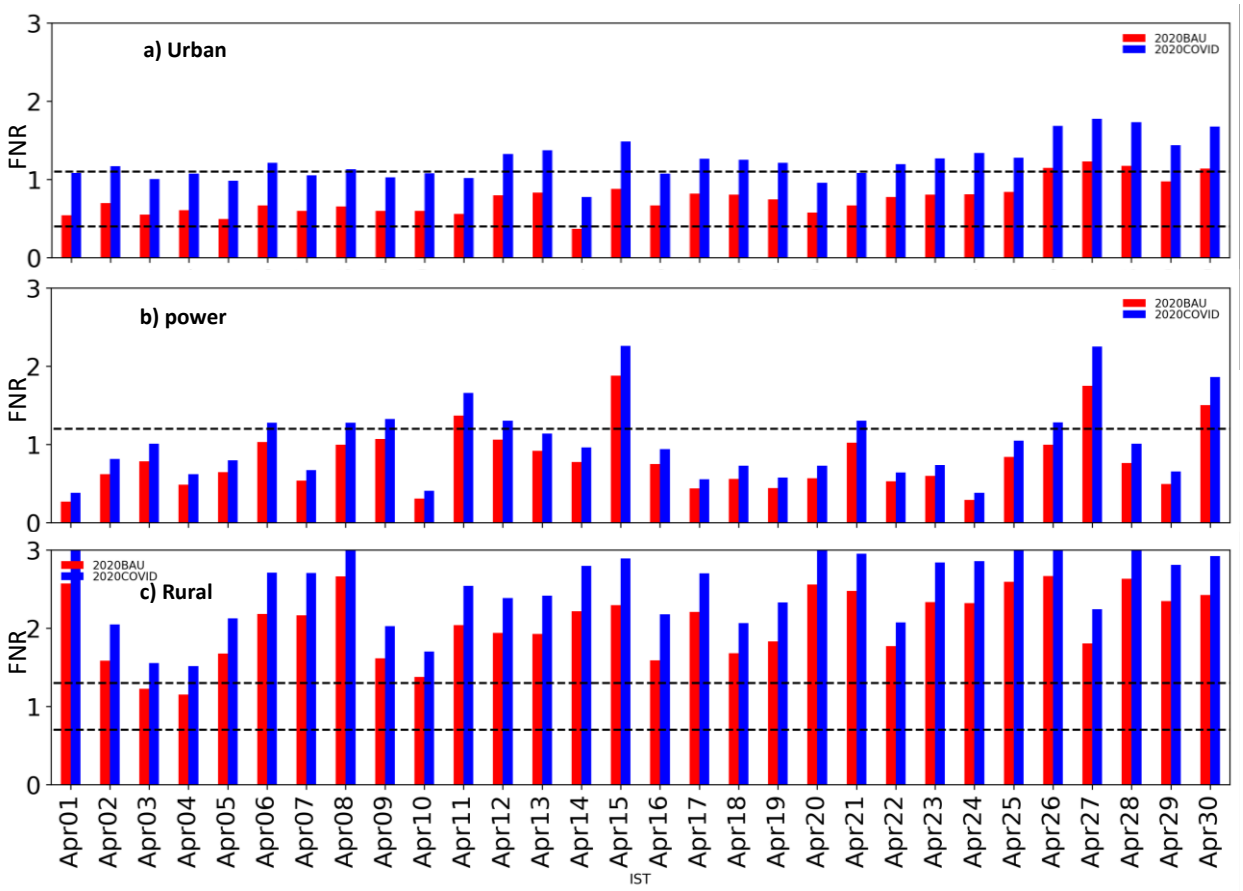

Figure 13 FNR ratio within the PBL averaged during afternoon (1230-1430 LT) in a) Urban, b) Power, and c) Rural regions. Dashed horizontal line in each panel represents the transition range calculated based on LROx/LNOx ratio analysis.

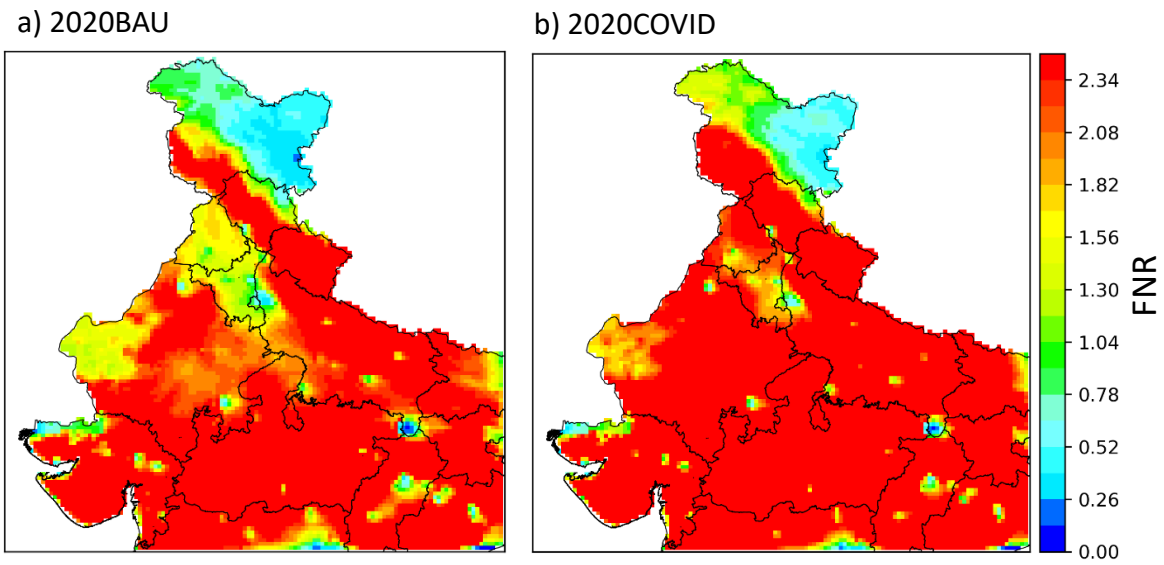

Figure 14 FNR ratio (within the PBL) averaged over April using a) 2020BAU and b) 2020COVID scenarios.

4. Summary and Conclusion

We studied the effects of COVID-19 stay-at-home orders (i.e. lockdown) on northern India's air quality and explored the chemistry behind the changes in ozone concentrations. For this purpose, we used the WRF-Chem version 4.0 model to utilize its integrated reaction rate (IRR) capability. The adjustment factors proposed by Doumbia et al. (2021) were used to account for the anthropogenic emission changes during the lockdown period in India. While the model satisfied the benchmark criteria proposed by Emery et al. (2017) for daily $PM_{2.5}$ concentration in Delhi, it overestimated (underestimated) the daytime ozone (NO_2 and CO) concentrations against the CPCB ground measurements data. However, the model was able to capture the overall observed trend in air pollutant concentrations in 2019 and 2020.

Four scenarios were designed to study the effect of the meteorology and lockdown anthropogenic emission perturbations in April 2019 and 2020. We found that the effects of perturbing the anthropogenic emissions could be different depending on the applied year. The reason is that not only the anthropogenic emissions but also the meteorological dependent emissions (e.g. biogenic emissions) and the atmospheric dynamics affect the air quality in a region. We also estimated the changes in air pollutant concentrations between April 2019 and 2020 and the contribution of meteorology and lockdown emissions. While the $PM_{2.5}$ concentration averaged over the IGP decreased by 6% in April 2020 due to the meteorology, it increased in the central India due to more biomass burning emissions. However, the lockdown emissions decreased the $PM_{2.5}$ concentration over Indian parts of the domain by 9%. For ozone, we found the meteorology decreased the concentrations over the IGP and increased it over the central India, similar to $PM_{2.5}$. However, the ozone concentration response to its precursors (i.e. NO_2 and VOCs) significant reductions due to the lockdown emissions was not constant over the domain. While ozone decreased in most parts of the domain, we saw that major cities like Delhi and the regions with many power plants showed increases in ozone with decreases in NOx emissions.

We also analyzed the ozone chemistry in an urban, a rural, and a densely populated power plants region during a sampled pre-lockdown and lockdown day. Using OH reactivity with VOCs (NO_2) as the pathway to ozone formation (destruction), we found that the lockdown emissions decreased both pathways in the

urban and rural region. However, it only decreased the ozone destruction in the power plant region (NO2+OH) and did not affect the ozone formation path (VOC+OH), as natural emission sources dominated the VOC emissions in this region. Our analysis showed that CO had the highest contribution in the net ozone production in all the regions and all the scenarios. We also found formaldehyde, isoprene, acetaldehyde, and ethylene contributed to the ozone formation in all the regions. However, the magnitude of contribution depended on the region and scenario. While formaldehyde was the second ranked VOC in the urban region in a business as usual scenario in 2020, isoprene had larger contribution in the lockdown scenario, indicating the impact of biogenic emissions in that region. We also found higher alkanes and higher alkenes, as tracers of anthropogenic emissions, contributed to the ozone formation in the rural region, indicating the effect of the transport in ozone formation.

Furthermore, we calculated the rates that radicals (i.e. HO_2 and RO_2) react with radicals (i.e. LROx) or NO_2 (i.e. LNOx) and used their ratio (LROx/LNOx) to find the ozone chemistry regime in different regions. Our analysis showed that the urban and power plant regions were primarily VOC-limited (LROx/LNOx <0.35), while the rural region was in NOx-limited region. Following Schroeder et al. (2017), we also calculated this ratio's corresponding formaldehyde to NO_2 concentration ratio (FNR) in each region. This is preferred as it can be calculated using ground measurements and satellite observation data. Our analysis suggested the FNR ratio of 1.3 as the upper-limit of the transition regime from VOC-limited to NOx-limited over India. Using that threshold, we classified most parts of India in the NOx-limited regime while most of the cities like Delhi and power plant region are in the VOC-limited regime. Some regions like the western IGP were towards the VOC-limited regime but shifted to NOx-limited regime after applying the lockdown emissions.

Understanding the ozone formation chemistry and the role of emission sources and different species can help the policy makers to implement efficient emission control scenarios. Our results showed that the ozone formation process can be different in each region depending on its local anthropogenic and natural emission sources and the meteorology. We acknowledge that our study was limited to only three arbitrary chosen regions. While our results can provide information on overall response of the air quality to emission reductions, they do not necessarily represent the general ozone chemistry in India. However, it provides a framework that can be used to study the efficacy of local emission control scenarios on ozone formation in India.

Data Availability

The WRF-Chem and IRR hourly output results for all four scenarios are available from Iowa Research Online at https://doi.org/10.25820/data.006144. TROPOMI data can be freely downloaded from the European Space Agency Copernicus Open Access Hub (https://doi.org/10.5270/S5P-s4ljg54). MERRA-2 data can be freely downloaded from NASA EarthData Portal (https://earthdata.nasa.gov/).

Acknowledgements

This work was funded in part by NASA HAQAST and ACMAP projects under awards NNX16AQ19G and 80NSSC19K094, respectively. BR also acknowledges supports from the university of Iowa graduate college summer fellowship. All the calculations and simulations are done using the University of Iowa Argon high-performance computing cluster. BR and GRC designed the research; BR performed all the model simulations; SKG provided measurements data; BR and MAO analyzed the IRR outputs. BR and GRC wrote the paper. All authors contributed to discussion and edited the paper. The authors declare that they have no conflict of interest.

References

Abdi-Oskouei, M., Pfister, G., Flocke, F., Sobhani, N., Saide, P., Fried, A., Richter, D., Weibring, P., Walega, J., & Carmichael, G. (2018). Impacts of physical parameterization on prediction of ethane concentrations for oil and gas emissions in WRF-Chem. *Atmospheric Chemistry and Physics, 18*(23), 16863-16883.

Amann, M., Kiesewetter, G., Schöpp, W., Klimont, Z., Winiwarter, W., Cofala, J., Rafaj, P., Höglund-Isaksson, L., Gomez-Sabriana, A., & Heyes, C. (2020). Reducing global air pollution: the scope for further policy interventions. *Philosophical Transactions of the Royal Society A, 378*(2183), 20190331.

Beig, G., Korhale, N., Rathod, A., Maji, S., Sahu, S. K., Dole, S., Latha, R., & Murthy, B. (2021). On modelling growing menace of household emissions under COVID-19 in Indian metros. *Environmental pollution, 272*, 115993.

Biswal, A., Singh, V., Singh, S., Kesarkar, A. P., Ravindra, K., Sokhi, R. S., Chipperfield, M. P., Dhomse, S. S., Pope, R. J., & Singh, T. (2020). COVID-19 lockdown induced changes in NO 2 levels across India observed by multi-satellite and surface observations. *Atmospheric Chemistry and Physics Discussions*, 1-28.

Bosilovich, M., Lucchesi, R., & Suarez, M. (2015). MERRA-2: File specification.

Chen, Y., Beig, G., Archer-Nicholls, S., Drysdale, W., Acton, W. J. F., Lowe, D., Nelson, B., Lee, J., Ran, L., & Wang, Y. (2020). Avoiding high ozone pollution in Delhi, India. *Faraday Discussions*.

Conibear, L. (2018). *Ambient air quality and human health in India.* (Doctor of Philosophy), University of Leeds, University of Leeds.

Conibear, L., Butt, E. W., Knote, C., Spracklen, D. V., & Arnold, S. R. (2018). Current and Future Disease Burden From Ambient Ozone Exposure in India. *GeoHealth, 2*(11), 334-355.

Doumbia, T., Granier, C., Elguindi, N., Bouarar, I., Darras, S., Brasseur, G., Gaubert, B., Liu, Y., Shi, X., & Stavrakou, T. (2021). Changes in global air pollutant emissions during the COVID-19 pandemic: a dataset for atmospheric chemistry modeling. *Earth System Science Data Discussions*, 1-26.

Dumka, U., Kaskaoutis, D., Verma, S., Ningombam, S. S., Kumar, S., & Ghosh, S. (2021). Silver linings in the dark clouds of COVID-19: Improvement of air quality over India and Delhi metropolitan area from measurements and WRF-CHIMERE model simulations. *Atmospheric Pollution Research, 12*(2), 225-242.

Duncan, B. N., Yoshida, Y., Olson, J. R., Sillman, S., Martin, R. V., Lamsal, L., Hu, Y., Pickering, K. E., Retscher, C., & Allen, D. J. (2010). Application of OMI observations to a space-based indicator of NOx and VOC controls on surface ozone formation. *Atmospheric Environment, 44*(18), 2213-2223.

Emery, C., Liu, Z., Russell, A. G., Odman, M. T., Yarwood, G., & Kumar, N. (2017). Recommendations on statistics and benchmarks to assess photochemical model performance. *Journal of the Air & Waste Management Association, 67*(5), 582-598.

Emery, C., Tai, E., & Yarwood, G. (2001). Enhanced meteorological modeling and performance evaluation for two Texas ozone episodes. *Prepared for the Texas natural resource conservation commission, by ENVIRON International Corporation*.

Emmons, L. K., Schwantes, R. H., Orlando, J. J., Tyndall, G., Kinnison, D., Lamarque, J. F., Marsh, D., Mills, M. J., Tilmes, S., & Bardeen, C. (2020). The chemistry mechanism in the Community Earth System Model version 2 (CESM2). *Journal of Advances in Modeling Earth Systems, 12*(4).

Emmons, L. K., Walters, S., Hess, P. G., Lamarque, J.-F., Pfister, G. G., Fillmore, D., Granier, C., Guenther, A., Kinnison, D., & Laepple, T. (2010). Description and evaluation of the Model for Ozone and Related chemical Tracers, version 4 (MOZART-4).

ESA. (2020). Air pollution drops in India following lockdown. Retrieved from https://www.esa.int/Applications/Observing_the_Earth/Copernicus/Sentinel-5P/Air_pollution_drops_in_India_following_lockdown#.YFzj-71W1ss.link

Garaga, R., Sahu, S. K., & Kota, S. H. (2018). A review of air quality modeling studies in India: local and regional scale. *Current Pollution Reports, 4*(2), 59-73.

Gaubert, B., Bouarar, I., Doumbia, T., Liu, Y., Stavrakou, T., Deroubaix, A. M., Darras, S., Elguindi, N., Granier, C., & Lacey, F. G. (2020). Global Changes in Secondary Atmospheric Pollutants during the 2020 COVID-19 Pandemic. *Earth and Space Science Open Archive ESSOAr*.

Ghude, S. D., Chate, D., Jena, C., Beig, G., Kumar, R., Barth, M., Pfister, G., Fadnavis, S., & Pithani, P. (2016). Premature mortality in India due to PM2. 5 and ozone exposure. *Geophysical Research Letters, 43*(9), 4650-4658.

Ghude, S. D., Jena, C., Chate, D., Beig, G., Pfister, G., Kumar, R., & Ramanathan, V. (2014). Reductions in India's crop yield due to ozone. *Geophysical Research Letters, 41*(15), 5685-5691.

Gkatzelis, G. I., Gilman, J. B., Brown, S. S., Eskes, H., Gomes, A. R., Lange, A. C., McDonald, B. C., Peischl, J., Petzold, A., Thompson, C. R., & Kiendler-Scharr, A. (2021). The global impacts of COVID-19 lockdowns on urban air pollution: A critical review and recommendations. *Elementa: Science of the Anthropocene, 9*(1). doi:10.1525/elementa.2021.00176

Goldberg, D. L., Anenberg, S. C., Griffin, D., McLinden, C. A., Lu, Z., & Streets, D. G. (2020). Disentangling the impact of the COVID-19 lockdowns on urban NO2 from natural variability. *Geophysical Research Letters, 47*(17), e2020GL089269.

Goldberg, D. L., Saide, P. E., Lamsal, L. N., Foy, B. d., Lu, Z., Woo, J.-H., Kim, Y., Kim, J., Gao, M., & Carmichael, G. (2019). A top-down assessment using OMI NO 2 suggests an underestimate in the NO x emissions inventory in Seoul, South Korea, during KORUS-AQ. *Atmospheric Chemistry and Physics, 19*(3), 1801-1818.

Gorris, M. E., Anenberg, S. C., Goldberg, D. L., Kerr, G. H., Stowell, J. D., Tong, D., & Zaitchik, B. F. (2021). Shaping the future of science: COVID-19 highlighting the importance of GeoHealth. *Earth and Space Science Open Archive ESSOAr*.

Granier, C., Darras, S., van der Gon, H. D., Jana, D., Elguindi, N., Bo, G., Michael, G., Marc, G., Jalkanen, J.-P., & Kuenen, J. (2019). *The Copernicus atmosphere monitoring service global and regional emissions (April 2019 version)*. Copernicus Atmosphere Monitoring Service,

Grell, G. A., Peckham, S. E., Schmitz, R., McKeen, S. A., Frost, G., Skamarock, W. C., & Eder, B. (2005). Fully coupled "online" chemistry within the WRF model. *Atmospheric Environment, 39*(37), 6957-6975.

Guenther, A., Karl, T., Harley, P., Wiedinmyer, C., Palmer, P., & Geron, C. (2006). Estimates of global terrestrial isoprene emissions using MEGAN (Model of Emissions of Gases and Aerosols from Nature). *Atmospheric Chemistry and Physics, 6*(11), 3181-3210.

Gupta, S. (2020). Air pollution in northern India has hit a 20-year low, NASA report says. *CNN*.

HEI. (2018). *Burden of Disease Attributable to Major Air Pollution Sources in India*. Retrieved from

Hodzic, A., & Jimenez, J. (2011). Modeling anthropogenically controlled secondary organic aerosols in a megacity: A simplified framework for global and climate models. *Geoscientific Model Development, 4*(4), 901-917.

Hodzic, A., Madronich, S., Kasibhatla, P., Tyndall, G., Aumont, B., Jimenez, J., Lee-Taylor, J., & Orlando, J. (2015). Organic photolysis reactions in tropospheric aerosols: effect on secondary organic aerosol formation and lifetime. *Atmospheric Chemistry and Physics, 15*(16), 9253-9269.

Jain, S., & Sharma, T. (2020). Social and travel lockdown impact considering coronavirus disease (COVID-19) on air quality in megacities of India: Present benefits, future challenges and way forward. *Aerosol and air quality research, 20*(6), 1222-1236.

Janssens-Maenhout, G., Crippa, M., Guizzardi, D., Dentener, F., Muntean, M., Pouliot, G., Keating, T., Zhang, Q., Kurokawa, J., & Wankmüller, R. (2015). HTAP_v2. 2: a mosaic of regional and global emission grid maps for 2008 and 2010 to study hemispheric transport of air pollution. *Atmospheric Chemistry and Physics, 15*(19), 11411-11432.

Jena, C., Ghude, S. D., Kulkarni, R., Debnath, S., Kumar, R., Soni, V. K., Acharja, P., Kulkarni, S. H., Khare, M., & Kaginalkar, A. J. (2020). Evaluating the sensitivity of fine particulate matter (PM 2.5) simulations to chemical mechanism in Delhi. *Atmospheric Chemistry and Physics Discussions*, 1-28.

Jin, X., & Holloway, T. (2015). Spatial and temporal variability of ozone sensitivity over China observed from the Ozone Monitoring Instrument. *Journal of Geophysical Research: Atmospheres, 120*(14), 7229-7246.

Knote, C., Hodzic, A., Jimenez, J., Volkamer, R., Orlando, J., Baidar, S., Brioude, J., Fast, J., Gentner, D., & Goldstein, A. (2014). Simulation of semi-explicit mechanisms of SOA formation from glyoxal in aerosol in a 3-D model. *Atmospheric Chemistry and Physics, 14*(12), 6213-6239.

Kota, S. H., Guo, H., Myllyvirta, L., Hu, J., Sahu, S. K., Garaga, R., Ying, Q., Gao, A., Dahiya, S., & Wang, Y. (2018). Year-long simulation of gaseous and particulate air pollutants in India. *Atmospheric Environment, 180*, 244-255.

Kumar, R., Barth, M., Pfister, G., Naja, M., & Brasseur, G. (2014). WRF-Chem simulations of a typical pre-monsoon dust storm in northern India: influences on aerosol optical properties and radiation budget. *Atmos. Chem. Phys, 14*(5), 2431-2446.

Kumar, R., Naja, M., Pfister, G., Barth, M., Wiedinmyer, C., & Brasseur, G. (2012). Simulations over South Asia using the Weather Research and Forecasting model with Chemistry (WRF-Chem): chemistry evaluation and initial results. *Geoscientific Model Development, 5*(3), 619-648.

Kumar, V., Beirle, S., Dörner, S., Mishra, A. K., Donner, S., Wang, Y., Sinha, V., & Wagner, T. (2020). Long-term MAX-DOAS measurements of NO 2, HCHO, and aerosols and evaluation of corresponding satellite data products over Mohali in the Indo-Gangetic Plain. *Atmospheric Chemistry and Physics, 20*(22), 14183-14235.

Kumari, P., & Toshniwal, D. (2020). Impact of lockdown measures during COVID-19 on air quality–A case study of India. *International journal of environmental health research*, 1-8.

Mahajan, A. S., De Smedt, I., Biswas, M. S., Ghude, S., Fadnavis, S., Roy, C., & van Roozendael, M. (2015). Inter-annual variations in satellite observations of nitrogen dioxide and formaldehyde over India. *Atmospheric Environment, 116*, 194-201.

Mahato, S., Pal, S., & Ghosh, K. G. (2020). Effect of lockdown amid COVID-19 pandemic on air quality of the megacity Delhi, India. *Science of the total environment, 730*, 139086.

Martin, R. V., Fiore, A. M., & Van Donkelaar, A. (2004). Space-based diagnosis of surface ozone sensitivity to anthropogenic emissions. *Geophysical Research Letters, 31*(6).

Miyazaki, K., Bowman, K., Sekiya, T., Takigawa, M., Neu, J. L., Sudo, K., Osterman, G., & Eskes, H. (2020). Global tropospheric ozone responses to reduced NOx emissions linked to the COVID-19 world-wide lockdowns. *Earth and Space Science Open Archive ESSOAr*.

Mor, S., Kumar, S., Singh, T., Dogra, S., Pandey, V., & Ravindra, K. (2021). Impact of COVID-19 lockdown on air quality in Chandigarh, India: understanding the emission sources during controlled anthropogenic activities. *Chemosphere, 263*, 127978.

Pfister, G., Wang, C. T., Barth, M., Flocke, F., Vizuete, W., & Walters, S. (2019). Chemical Characteristics and Ozone Production in the Northern Colorado Front Range. *Journal of Geophysical Research: Atmospheres, 124*(23), 13397-13419.

Pommier, M., Fagerli, H., Gauss, M., Simpson, D., Sharma, S., Sinha, V., Ghude, S. D., Landgren, O., Nyiri, A., & Wind, P. (2018). Impact of regional climate change and future emission scenarios on surface O 3 and PM 2.5 over India. *Atmospheric Chemistry and Physics, 18*(1), 103-127.

Pusede, S., & Cohen, R. (2012). On the observed response of ozone to NO x and VOC reactivity reductions in San Joaquin Valley California 1995–present. *Atmospheric Chemistry and Physics, 12*(18), 8323-8339.

Roozitalab, B., Carmichael, G. R., & Guttikunda, S. K. (2021). Improving regional air quality predictions in the Indo-Gangetic Plain–case study of an intensive pollution episode in November 2017. *Atmospheric Chemistry and Physics, 21*(4), 2837-2860.

Sarkar, S., Chauhan, A., Kumar, R., & Singh, R. P. (2019). Impact of deadly dust storms (May 2018) on air quality, meteorological, and atmospheric parameters over the northern parts of India. *GeoHealth, 3*(3), 67-80.

Schroeder, J. R., Crawford, J. H., Fried, A., Walega, J., Weinheimer, A., Wisthaler, A., Müller, M., Mikoviny, T., Chen, G., & Shook, M. (2017). New insights into the column CH2O/NO2 ratio as an indicator of near-surface ozone sensitivity. *Journal of Geophysical Research: Atmospheres, 122*(16), 8885-8907.

Seinfeld, J. H., & Pandis, S. N. (2016). *Atmospheric chemistry and physics: from air pollution to climate change*: John Wiley & Sons.

Selvam, S., Muthukumar, P., Venkatramanan, S., Roy, P., Bharath, K. M., & Jesuraja, K. (2020). SARS-CoV-2 pandemic lockdown: effects on air quality in the industrialized Gujarat state of India. *Science of the total environment, 737*, 140391.

Sharma, A., Ojha, N., Pozzer, A., Mar, K. A., Beig, G., Lelieveld, J., & Gunthe, S. S. (2017). WRF-Chem simulated surface ozone over south Asia during the pre-monsoon: effects of emission inventories and chemical mechanisms. *Atmospheric Chemistry and Physics, 17*(23), 14393-14413.

Shi, X., & Brasseur, G. P. (2020). The response in air quality to the reduction of Chinese economic activities during the COVID-19 outbreak. *Geophysical Research Letters, 47*(11), e2020GL088070.

Sicard, P., De Marco, A., Agathokleous, E., Feng, Z., Xu, X., Paoletti, E., Rodriguez, J. J. D., & Calatayud, V. (2020). Amplified ozone pollution in cities during the COVID-19 lockdown. *Science of the total environment, 735*, 139542.

Sillman, S. (1995). The use of NO y, H2O2, and HNO3 as indicators for ozone-NO x-hydrocarbon sensitivity in urban locations. *Journal of Geophysical Research: Atmospheres, 100*(D7), 14175-14188.

Singh, V., Singh, S., Biswal, A., Kesarkar, A. P., Mor, S., & Ravindra, K. (2020). Diurnal and temporal changes in air pollution during COVID-19 strict lockdown over different regions of India. *Environmental pollution, 266*, 115368.

Souri, A. H., Chance, K., Bak, J., Nowlan, C. R., González Abad, G., Jung, Y., Wong, D. C., Mao, J., & Liu, X. (2021). Unraveling Pathways of Elevated Ozone Induced by the 2020 Lockdown in Europe by an Observationally Constrained Regional Model: Non-Linear Joint Inversion of NO x and VOC Emissions using TROPOMI. *Atmospheric Chemistry and Physics Discussions*, 1-45.

Souri, A. H., Nowlan, C. R., Wolfe, G. M., Lamsal, L. N., Miller, C. E. C., Abad, G. G., Janz, S. J., Fried, A., Blake, D. R., & Weinheimer, A. J. (2020). Revisiting the effectiveness of HCHO/NO2 ratios for inferring ozone sensitivity to its precursors using high resolution airborne remote sensing observations in a high ozone episode during the KORUS-AQ campaign. *Atmospheric Environment, 224*, 117341.

Srinivas, R., Beig, G., & Peshin, S. K. (2016). Role of transport in elevated CO levels over Delhi during onset phase of monsoon. *Atmospheric Environment, 140*, 234-241.

Vadrevu, K. P., Eaturu, A., Biswas, S., Lasko, K., Sahu, S., Garg, J., & Justice, C. (2020). Spatial and temporal variations of air pollution over 41 cities of India during the COVID-19 lockdown period. *Scientific reports, 10*(1), 1-15.

Whole Atmosphere Community Climate Model (WACCM) Model Output. (2020). Retrieved from: https://rda.ucar.edu/datasets/ds313.6/

Wiedinmyer, C., Akagi, S., Yokelson, R. J., Emmons, L., Al-Saadi, J., Orlando, J., & Soja, A. (2011). The Fire INventory from NCAR (FINN): A high resolution global model to estimate the emissions from open burning. *Geoscientific Model Development, 4*(3), 625.

Yadav, R., Korhale, N., Anand, V., Rathod, A., Bano, S., Shinde, R., Latha, R., Sahu, S., Murthy, B., & Beig, G. (2020). COVID-19 lockdown and air quality of SAFAR-India metro cities. *Urban Climate, 34*, 100729.

Zaveri, R. A., Easter, R. C., Fast, J. D., & Peters, L. K. (2008). Model for simulating aerosol interactions and chemistry (MOSAIC). *Journal of Geophysical Research: Atmospheres, 113*(D13).

Zhang, M., Katiyar, A., Zhu, S., Shen, J., Xia, M., Ma, J., Kota, S. H., Wang, P., & Zhang, H. (2021). Impact of reduced anthropogenic emissions during COVID-19 on air quality in India. *Atmospheric Chemistry and Physics*, *21*(5), 4025-4037.

References from the Supporting Information

Guttikunda, S. K., Nishadh, K., and Jawahar, P.: Air pollution knowledge assessments (APnA) for 20 Indian cities, Urban Climate, 27, 124-141, 2019.

Jena, C., Ghude, S. D., Kumar, R., Debnath, S., Govardhan, G., Soni, V. K., Kulkarni, S. H., Beig, G., Nanjundiah, R. S., and Rajeevan, M.: Performance of high resolution (400 m) PM 2.5 forecast over Delhi, Scientific reports, 11, 1-9, 2021.